Low Cost Gas Turbine Off-Design Prediction Technique

by

Jeremy Martinjako

A Thesis Presented in Partial Fulfillment
of the Requirements for the Degree
Master of Science

Approved April 2014 by the
Graduate Supervisor Committee:

Steven Trimble, Chair
Werner Dahm
James Middleton

ARIZONA STATE UNIVERSITY

May 2014

ABSTRACT

This thesis seeks to further explore off-design point operation of gas turbines and to examine the capabilities of GasTurb 12 as a tool for off-design analysis. It is a continuation of previous thesis work which initially explored the capabilities of GasTurb 12. The research is conducted in order to: 1) validate GasTurb 12 and, 2) predict off-design performance of the Garrett GTCP85-98D located at the Arizona State University Tempe campus.

GasTurb 12 is validated as an off-design point tool by using the program to predict performance of an LM2500+ marine gas turbine. Haglind and Elmegaard (2009) published a paper detailing a second off-design point method and it includes the manufacturer's off-design point data for the LM2500+. GasTurb 12 is used to predict off-design point performance of the LM2500+ and compared to the manufacturer's data. The GasTurb 12 predictions show good correlation.

Garrett has published specification data for the GTCP85-98D. This specification data is analyzed to determine the design point and to comment on off-design trends.

Arizona State University GTCP85-98D off-design experimental data is evaluated. Trends presented in the data are commented on and explained. The trends match the expected behavior demonstrated in the specification data for the same gas turbine system.

It was originally intended that a model of the GTCP85-98D be constructed in GasTurb 12 and used to predict off-design performance. The prediction would be compared to collected experimental data. This is not possible because the free version of GasTurb 12 used in this research does not have a module to model a single spool turboshaft. This module needs to be purchased for this analysis.

TABLE OF CONTENTS

Page

CHAPTER Page

APPENDIX Page

LIST OF TABLES

LIST OF FIGURES

Figure Page

NOMENCLATURE

T	Temperature (K)
P	Pressure (kPa)
ṁ	Mass Flow Rate $\left(\frac{kg}{s}\right)$
LHV	Lower Heating Value $\left(\frac{kJ}{kg}\right)$
ρ	Density $\left(\frac{kg}{m^3}\right)$
R	Ideal Gas Constant $\left(\frac{J}{mol\ K}\right)$
γ	Heat Capacity Ratio
h	Enthalpy $\left(\frac{kJ}{kg\ K}\right)$
η	Efficiency
c_p	Specific Heat $\left(\frac{kJ}{kg}\right)$
$\dot{V}$	Volumetric Flow Rate $\left(\frac{m^3}{s}\right)$

1. Introduction

The research presented in this thesis seeks to further explore off-design point operation of gas turbines and to examine the capabilities of GasTurb 12 as a tool for off-design analysis. Previous work (Martinjako 2013) has shown that GasTurb 12 provides good results for a Brayton cycle analysis of a gas turbine when compared to theoretical design point results using a complex analysis method and has suggested that GasTurb12 can be used to predict off-design point performance of a gas turbine. The results are inconclusive because they do not compare a GasTurb 12 prediction to experimental off-design data.

The purpose of this research is to determine if GasTurb 12 provides off-design results with good correlation to experimental results. There is a gas turbine setup at Arizona State University which is used to gather experimental data at off-design point operating conditions. The gas turbine is a Garrett GTCP85-89D which is outfitted with a data acquisition system in a typical lab setup in order to collect experimental data. The setup is explained in detail in chapter 5.

In order to verify the accuracy of predictions made with GasTurb 12, it is necessary to first compare an off-design point prediction in GasTurb 12 with known off-design point data. Haglind and Elmegaard (2009) published a paper with off-design results for a GE LM2500+ gas turbine and these results will be used to create a model of the LM2500+ in GasTurb 12. A comparison will be made in order to validate the off-design predictions.

A model of the GTCP85-98D will be made in GasTurb 12. Experimental data will be analyzed in order to evaluate the performance of the GTCP85 at off-design conditions and the GasTurb 12 model will be used to predict off-design performance of the GTCP85-98D. The predictions will be compared to experimental results to determine how well GasTurb 12 predictions correlate to experimental off-design performance of the GTCP85-98D.

1.1 Research Questions

The experimental deliverables described above lead to the following research questions:

1. How well does GasTurb 12 predict off-design point performance of an existing, documented, non-bleed gas turbine?
2. What are the characteristics of a bleed-air APU gas turbine in general and the GTCP85 specifically, including a cycle model?
3. How does the ASU GTCP85 test data compare with manufacturer's specification values for this engine?
4. Can the current GasTurb 12 software package be used to predict GTCP85 performance to compare with published specification data?
5. How does the ASU GTCP85 test data for no bleed compare with the GasTurb 12 model?
6. What are the next steps to model the GTCP85 with bleed?

1.2 Background

1.2.1 Gas Turbine Configurations

The research presented herein deals with two configurations of gas turbine systems. The LM2500+ is a two spool turboshaft system connected to a generator and used to generate electrical power. It has minimal bleed air extracted for cooling purposes and is used as a power source for marine applications. As the name implies, two-spool turboshaft systems feature two separate spools. The first spool connects the compressor and the high pressure turbine, in a part of the system known as the gas generator. The second spool connects the power turbine to a load cell or generator. The high pressure turbine only extracts enough power from the expanding exhaust products to run the compressor and the rest is allowed to fully expand across the power turbine in order to power a generator. Figure 1.1 shows the general layout of a two-spool turboshaft system and figure 1.2 shows a picture of the LM2500+.

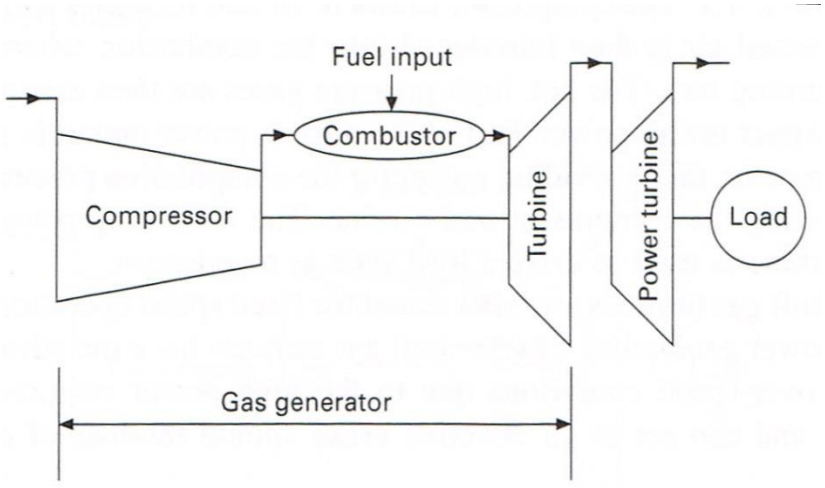

Figure 1.1. A typical two-spool turboshaft layout (Rezak 2007).

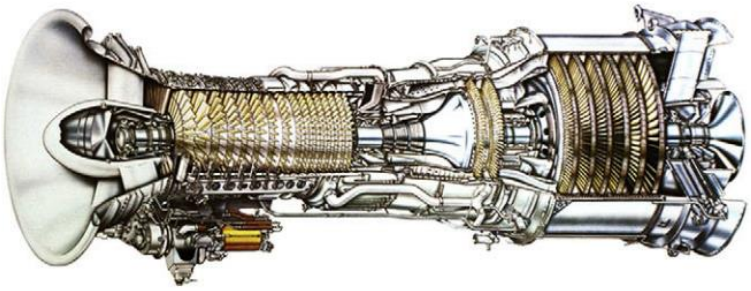

Figure 1.2. The LM2500+ (Haglind & Elmegaard 2009).

The GTCP85-98D is a single spool turbine system. Unlike the LM2500+, it is designed to not only produce shaft power output, but also to provide compressed bleed air for pneumatic systems. The single spool connects the compressor, the turbine, and the load cell onto a single shaft which operates at a constant speed. Figure 1.3 shows the general layout of a single spool turbine system, and figure 1.4 shows a picture of the GTCP85-98D.

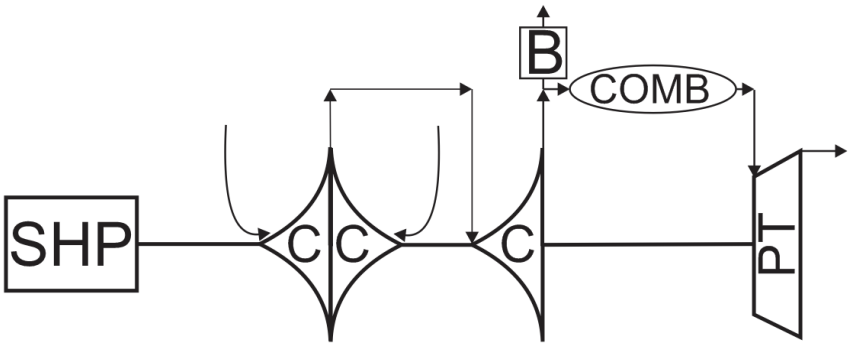

Figure 1.3. The layout of the GTCP85-98D. In the notation, "C" represents a centrifugal compressor, "B" represents a bleed air valve, "PT" represents the turbine, "COMB" represents the combustor, and "SHP" represents the load cell where shaft power is delivered.

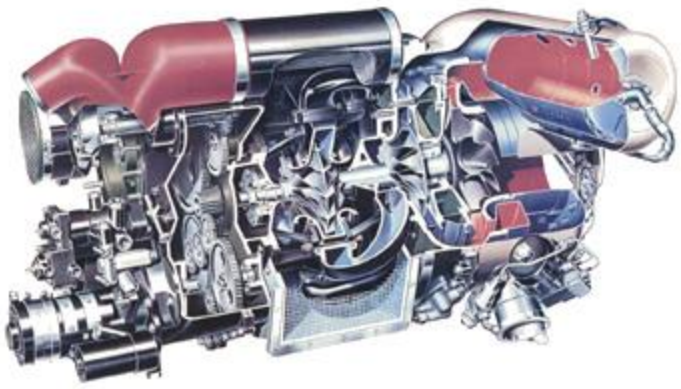

Figure 1.4. The GTCP85 (85 Series Auxiliary Power Unit 1969).

1.2.2 Fundamentals of Off-Design

Off-design point analysis is important because most gas turbines have an operational envelope and have to operate for some time outside of their design point. The design point represents the operating condition the gas turbine system is expected to operate at most often. This leads to a decrease in overall efficiency and is generally undesirable. The decrease in efficiency is a result of complex interplay between each component of a gas turbine system (Razak 2007). Each component of the gas turbine is individually characterized, but components are optimized such that they work well together at the design point. Complex components aside, this means that as the gas turbine deviates from its intended operating point, the components will no longer be optimized, and a loss in efficiency occurs. At extreme off-design conditions, the components may even cease to work together. One example of this is compressor surge. When the compressor experiences surge, it is operating at a point of aerodynamic instability and often parts of the compressor will stall, leading to greatly reduced

performance of the compressor (Bathie 1996). The reduced compressor performance will greatly impact subsequent component performance, and the system as a whole.

The most common off-design operating conditions are part power loading and variances in the operating point (Walsh and Fletcher 1998). These deviations from the design point cause the system to operate differently than intended and lead to decreased performance. Off-design is important in working with ground-based power turbines because although they may operate in the same location year round, they are subject to seasonal temperature changes and may have to operate at part power. It is important to understand how a gas turbine operates at off-design conditions and the reasons why.

A simple gas turbine system consists of a compressor, a combustor, and a turbine. Some configurations may have additional compressors, turbines, and other cycle modifiers, but at the root, all gas turbines have these three major components. Air enters the compressor where it is compressed; then passes through a combustor where energy is added to the compressed gas by the burning of fuel; and then the high pressure, hot exhaust products expand across a turbine to extract power. Each component is an individual piece and must be matched with all other components to create a working system. A well designed gas turbine system will have well matched components that work well together over the entire operating range.

Component performance is characterized with component maps. A component map typically plots pressure ratio versus a flow parameter. The flow parameter is most often non-dimensional flow or corrected flow. Both flow parameters are related; non-dimensional flow is proportional to corrected flow. Non-dimensional flow is given in equation 1.1 and corrected flow is given in equation 1.2 (Razak 2007).

$$NDF = \frac{\dot{m}_i\sqrt{T}}{P} \quad (1.1)$$

$$CF = \frac{\dot{m}_i\sqrt{\theta_t}}{\delta_t} \quad (1.2)$$

θ_t represents the ratio of total temperature at the inlet to standard temperature and δ_t represents the ratio of total pressure at the inlet to standard pressure. Both are defined in equations 1.3 and 1.4 and are unit-less.

$$\theta_t = \frac{T_1}{288.15} \quad (1.3)$$

$$\delta_t = \frac{P_1}{101.325} \quad (1.4)$$

The maps feature corrected speed lines which show operating lines at a constant corrected speed (equation 1.5), contours of constant isentropic efficiency, and a surge line. The surge line represents a limit in operation such that "above and to the left of the surge line, aerodynamic instabilities become greater than can be tolerated" and parts of the compressor will begin to stall (Bathie 1996). A surge line is common to a compressor map. A sample compressor map is shown in figure 1.5.

$$\mathrm{N_c} = \frac{\mathrm{N}}{\sqrt{\theta_t}} \quad (1.5)$$

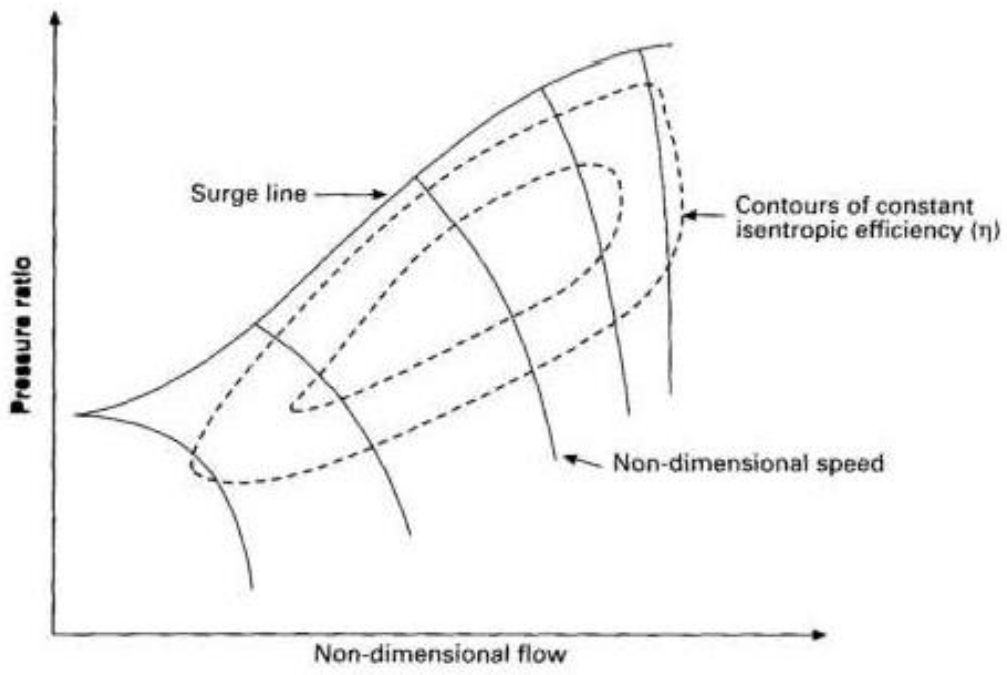

Figure 1.5. A typical compressor map.

The compressor map shows that if the compressor is operated at constant non-dimensional speed and non-dimensional flow increases, the operating point moves from the left to the right on the map along a non-dimensional speed line. As this movement occurs, the operating point passes through isentropic efficiency contours and the isentropic efficiency of the compressor will decrease. The pressure ratio across the compressor will also decrease. Eventually the compressor may also choke, as seen in figure 1.5 by vertical non-dimensional speed lines. Choked flow represents conditions in the gas turbine system where non-dimensional flow can no longer increase, but both pressure ratio and isentropic efficiency can continue to change (Bathie 1996).

Turbine performance is mapped in one of two ways. The first way is to use a map identical to a compressor map, which plots pressure ratio versus non-dimensional flow,

with constant non-dimensional speed lines and isentropic efficiency contours. An example of this is shown in figure 3.3. The second method is to use two separate plots, one which plots turbine efficiency versus expansion ratio, and the other which plots non-dimensional flow versus expansion ratio. These plots are made for constant non-dimensional speed lines and provide similar information to the turbine map. An example of these plots can be seen in figure 1.6 and 1.7. It should be noted that expansion ratio and pressure ratio are used interchangeably for the turbine and represent the ratio of pressures from the inlet of the turbine to the exit. An interesting characteristic in the plot of non-dimensional flow versus expansion ratio is that it shows clearly where the turbine chokes.

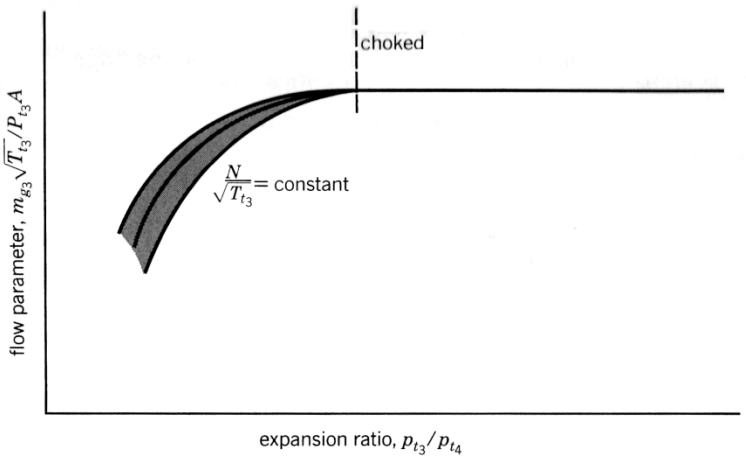

Figure 1.6. Non-dimensional flow of a turbine plotted versus the expansion ratio (Bathie 1996).

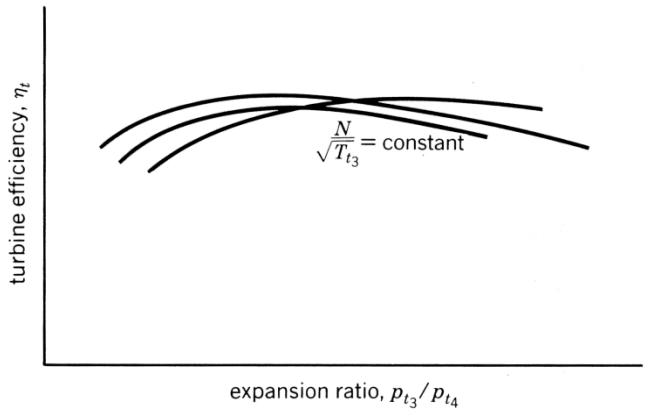

Figure 1.7. Turbine efficiency plotted versus the expansion ratio (Bathie 1996).

Choking is important in gas turbine operation. Often the turbine will choke and continuity demands that flow will then be limited through the entire system. In a two-spool configuration, the power turbine is often the limiting factor. It dictates operation for the high pressure turbine, because when multiple turbines operate in series, the swallowing capacity of the power turbine determines how the high pressure turbine will operate (Razak 2007). The power turbine chokes before the high pressure turbine does, and the high pressure turbine cannot pass more mass flow through than the power turbine may swallow. This is illustrated in figure 1.8.

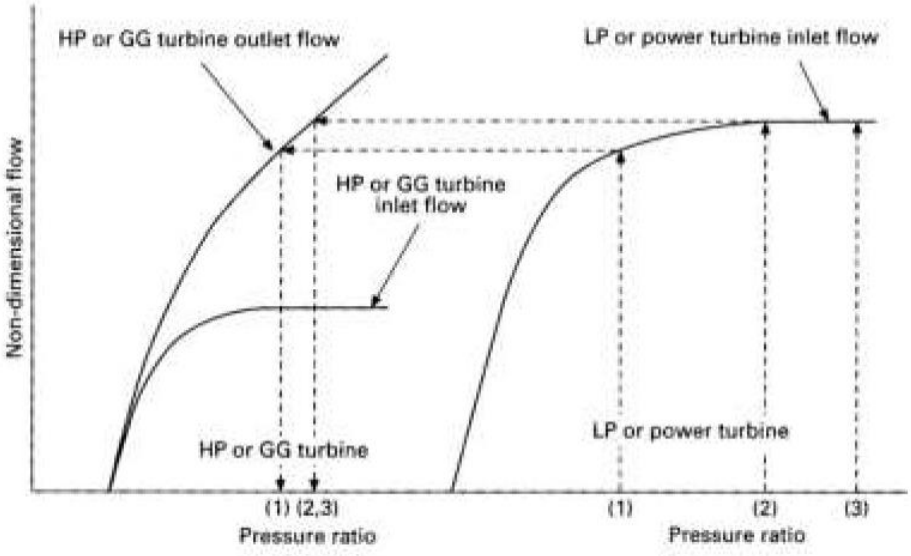

Figure 1.8. Performance of turbines operating in series. (1) denotes unchoked power turbine flow and (2)&(3) represent choked power turbine flow (Razak 2007).

1.2.3 Application to the LM2500+ and the GTCP85-98D

Component maps are important for off-design. They show how each component will operate at any point in its operating envelope. Off-design point analysis is performed by modeling an off-design point and calculating how each component operates at that condition and how the operation of each component affects subsequent components. The interaction of components means that a single spool system will operate differently than a two-spool system at off-design conditions. As a result, multiple modules are necessary in GasTurb 12 to model each gas turbine configuration; the single spool module will not accurately model a two-spool configuration, and vice versa.

A two-spool system, like the LM2500+, features a free gas generator which can respond to changes in operating conditions. It can speed up or slow down as needed to

maintain steady operation because it is not mechanically linked to the power turbine and is versatile over a range of operating conditions. This configuration is commonly used for power generation because it leads to smaller starting power requirements and better off-design performance (Razak 2007).

A single spool system, like the GTCP85-98D, is limited because the components are all fixed to a single shaft. The system is optimized to run at a single speed and cannot readily respond to changes in operating conditions. This results in good performance at maximum load, but poor off-design performance at part power conditions. It is expected the GTCP85-98D will most often be run at full power, trading off electric power generation for bleed air compression (85 Series Auxiliary Power Unit 1969).

2. Literature Review

2.1 Use-Inspired Research Needs

Feasibility studies and conceptual studies on gas turbine performance often do not include the effects of off-design operation on power output and fuel consumption. These are important effects for gas turbines that operate at off-design operating conditions. Arizona State University has a Garrett GTCP85-98D gas turbine that is in need of this characterization in order to show how the GTCP98-98D operates at off-design operating conditions. A low-cost, easy use method to perform off-design predictions is required.

2.2 Off-Design Analysis Methods

Common methods to predict off-design performance are complex analyses of the interplay of the large number of variables involved in component matching (Bathie 1996). These methods use component maps to determine the operational characteristics of each component for a given off-design condition and each component must be matched in such a way that the system operates with continuity at a steady state. The result is a tedious, iterative process to determine a single off-design point, requires a great deal of assumptions to be made, and is only accurate enough to offer a general idea of off-design performance. An example off-design analysis procedure is shown in figure 2.1.

The following discussion describes a general matching procedure. It is assumed that the flight conditions (altitude and velocity) and turbine inlet temperature are known.

1. Knowing the flight condition fixes T_{o1} and p_{o1}.
2. Assume an LPC operating point (assume $p_{o1.5}/p_{o1}$ and $\dot{m}_{a1}\sqrt{\theta_{o1}}/\delta_{o1}$. Since η_{LPC} and $N_{LPC}/\sqrt{\theta_{o1}}$ are known from the LPC map (Figure 10.7*a*), N_{LPC}, $\dot{m}_{a1}$, $\Delta h_{LPC,a}$, $\dot{m}_{a1.5}$, $T_{o1.5,a}$ and $p_{o1.5}$ may be calculated.
3. Assume an LPC pressure ratio, $p_{o2}/p_{o1.5}$. Calculate $\dot{m}_{a1.5}\sqrt{\theta_{o1.5}}/\delta_{o1.5}$, then read from the HPC map (Figure 10.7*b*) η_{HPC}, $N_{HPC}/\sqrt{\theta_{o1.5}}$. Calculate N_{HPC}, $\Delta h_{LPC,a}$, $\dot{m}_{a2}$, T_{o2a}, and p_{o2}.
4. Since T_{o3} is known, determine the fuel–air ratio and combustion chamber pressure drop. Calculate $\dot{m}_{g3}$ and p_{o3}.
5. Assume a HPT expansion ratio. Calculate $N_{HPT}/\sqrt{\theta_{o3}}$. Determine from the turbine performance characteristics η_{HPT} (Figure 10.7*d*) and $\dot{m}_{g3}\sqrt{T_{o3}}/p_{o3}A_3$ (Figure 10.7*c*). Calculate $\Delta h_{HPT,a}$ and $\dot{m}_{g3}$.
6. Check to determine if $\Delta h_{HPT,a}$ and $\dot{m}_{g3}$ are within a preset tolerance. If not, repeat steps 3 through 5 until a match does exist.
7. Once the high-pressure spool has been matched, $\dot{m}_{g3.5}$, $p_{o3.5}$, $T_{o3.5a}$, and N_{LPC} are known. Assume an LPT expansion ratio, $p_{o3.5}/p_{o4}$. Determine η_{LPC} (Figure 10.7*f*) and $\dot{m}_{g3.5}\sqrt{T_{o3.5}}/p_{o3.5}A_{3.5}$ (Figure 10.7*e*). Calculate $\Delta h_{LPT,a}$ and $\dot{m}_{g3.5}$.
8. Check to determine if $\Delta h_{LPT,a}$ and $\dot{m}_{g3}$ are within a preset tolerance. If not, repeat steps 2 through 7 until a match does exist.
9. Once the low-pressure spool has been matched, $\dot{m}_{g4}$, p_{o4}, and T_{o4a} are known. Determine, from the exhaust nozzle flow characteristics (Figure 10.7*g*), $\dot{m}_{g4}\sqrt{T_{o4}}/p_{o4}A_4$. Calculate A_4 and compare with the known exhaust nozzle A_4. An engine match exists and the thrust, thrust-specific fuel consumption, and other desired values may be calculated with a preset tolerance. If a match does not exist, repeat 2 through 9 until a match has been achieved.

Figure 2.1. An example off-design point analysis procedure (Bathie 1996).

These processes requires detailed component maps in order to determine the performance of each component at a given off-design point. Unfortunately components maps are not often available to the public as they are proprietary information used in design; they are not provided along with other specs. In the absence of detailed component maps or other crucial information, it is very difficult to perform off-design point analysis. Even with the information, the process is still tedious and only accurate to a first order (Walsh and Fletcher 1998). The large engine manufacturers have their own

in-house software to perform this sort of analysis to a high order of accuracy, but consumers and small scale engine designers do not have these sorts of tools readily available. This presents a need for a low-cost, simple to use method which can make accurate predictions without detailed component maps.

2.3 Low-Cost Off-Design Method

GasTurb 12 has been suggested as a simple to use tool to perform off-design point analysis, without the need of detailed component maps. It only requires a small number of typically used input parameters in order to generate a model of the gas turbine system and to calculate off-deign point predictions. Without detailed component maps the predictions are limited, but they can provide a good idea of off-design point operation characteristics in a quick and simple manner. The ability to perform simple off-design analysis without the need to acquire component maps or go into a tedious process is very beneficial to consumers and educators. It allows for a consumer to predict how a purchase may operate throughout the year or help an educator demonstrate off-design performance.

3. GasTurb 12 Model Description

GasTurb 12 is a computerized gas turbine software package that has been identified as a potentially useful tool to perform basic off-design point analysis of gas turbine systems. Previous thesis work sought to explore the nature of the program to determine how to use the program and what sort of outputs it can provide. The complete work can be found in "Simple Method for Estimating Shaft-Power Gas Turbine Off-Design Point Performance" (Martinjako 2013). A summary of the results is provided in sections 3.3 and 3.4.

3.1 Capabilities

GasTurb12 is a complete software package capable of performing design point and off-design point analyses, as well as more advanced analyses, for a variety of gas turbine configurations for use in both propulsion systems and for power generation. This work and the original exploration of GasTurb 12 use only the free version of the software package which features a limited tool set. In the free version of the software, only three configuration modules are enabled: a two-spool turboshaft for power generation, a turbojet, and a two-spool turbofan. This work is concerned with gas turbines used for power generation so only the two-spool turboshaft is of interest.

GasTurb 12 uses a number of known cycle parameters to create a model of a two-spool turboshaft at design point conditions. These parameters are: the inlet mass flow rate, $\dot{m}_i$; the pressure ratio, r_p; the burner exit temperature (also referred to as the turbine

inlet temperature), T_3; the lower heating value of the fuel, LHV; the bleed air mass flow rate, $\dot{m}_b$; the total inlet temperature, T_1; the total inlet pressure, P_1; the isentropic compressor efficiency, η_c; the isentropic high pressure turbine efficiency, η_{hpt}; the isentropic power turbine efficiency, η_{pt}; and the generator efficiency, η_g. A detailed user's manual describing how to set up the program can be found in Martinjako (2013).

Using the inputs described above, GasTurb 12 can provide a variety outputs. All functions within the program depend on a basic design point model which is created using the described input parameters. The design point model outputs the performance of the two-spool turboshaft at the design point, including: the temperature and pressure at each point within the system; the thermal efficiency, η_{th}; the mass flow rate of fuel, $\dot{m}_f$; and the power generated, $\dot{W}_g$. The design point tool can also be used to run parametric studies. Figure 3.1 shows the state points within the two-spool turboshaft model.

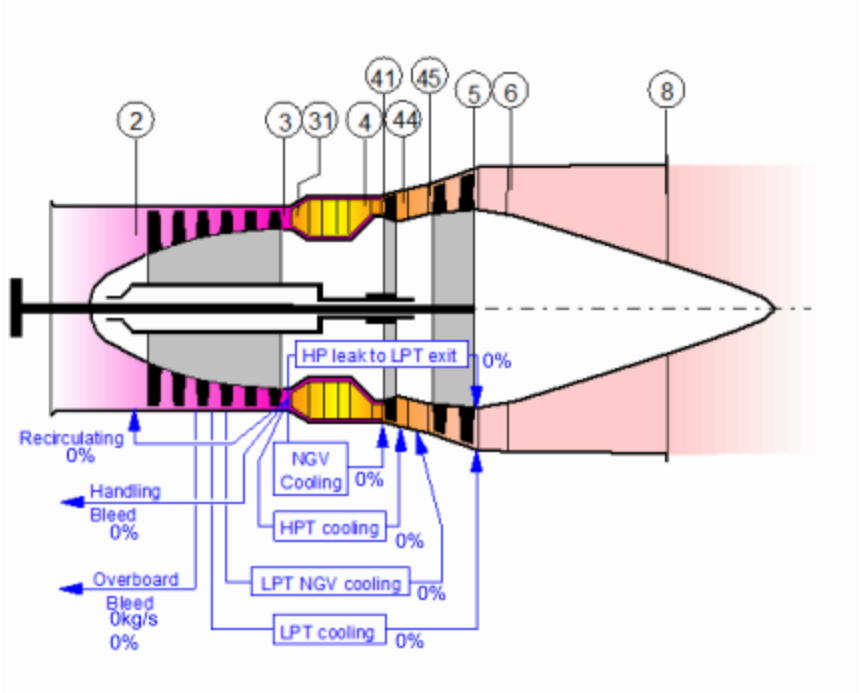

Figure 3.1. The state points within the two-spool turboshaft model used in GasTurb 12. The important points are the compressor inlet, point 2; the compressor exit, point 3; the high pressure turbine inlet, point 41; the low pressure turbine inlet, point 45; and the exhaust, point 5.

The primary interest to this work is the off-design tool. The off-design tool requires a design point model to be made first. The off-design tool can be used to calculate single off-design points by varying operating conditions within the interface. The tool can also be used to determine an operating line for the gas turbine system. The operating line can be run by either varying the gas generator speed or by varying the power output. In both cases, the design point is treated as the maximum power condition.

The operating line provides very useful information. It can generate plots of virtually any quantity of interest within the gas turbine system versus any abscissa. Each point along the operating line represents how the gas turbine system is expected to operate at that off-design point condition. It can further be used to generate compressor

and turbine maps which show all points along the operating line in each of the component maps. Examples of these component maps are provided in section 3.3. Table 3.1 shows all the necessary input parameters needed to create a design point model of a two-spool turboshaft as well as the possible outputs GasTurb 12 can provide.

Table 3.1. All input parameters needed to create a design point model of a two-spool turboshaft in GasTurb 12 alongside the possible outputs.

Input			Output		
Design Point			*Design Point*		
Input Parameter	**Symbol**	**Units**	**Output Parameter**	**Symbol**	**Units**
Inlet Mass Flow	$\dot{m}_i$	kg/s	Thermal Efficiency	η_{th}	-
Pressure Ratio	r_p	-	Fuel Mass Flow Rate	$\dot{m}_f$	kg/s
Burner Exit Temperature	T_3	K	Power Generated	$\dot{W}_g$	kW
Lower Heating Value of Fuel	LHV	MJ/kg	Parametric Studies	-	-
Bleed Mass Flow	$\dot{m}_b$	kg/s	*Off-Design*		
Ambient Temperature	T_1	K	Off-Design Points	-	-
Ambient Pressure	p_1	kPa	Off-Design Plots	-	-
Isentropic Compressor Efficiency	η_c	-	Compressor Map	-	-
Isentropic Turbine Efficiency	η_t	-	HP Turbine Map	-	-
Generator Efficiency	η_g	-	P Turbine Map	-	-

3.2 Validation

GasTurb 12 is validated in design point analysis by comparing results from the program with known, published results of a two-spool gas turbine system. GasTurb 12 is used to model a gas turbine described in a problem statement against an increasingly complex theoretical model presented in the literature (Bathie 1996), which first uses a simplified Brayton cycle analysis and goes on to use an increasingly more complex scheme to better approximate real operating conditions. An excerpt of the comparison is

shown in table 3.2. The design point values are very similar between the example problems and the GasTurb 12 calculations. They begin with some discrepancy, but as the example problem solution method becomes more complex, the results match much more closely. This suggests that GasTurb 12 uses a complex algorithm to perform Brayton cycle analysis which takes into consideration frictional losses, pressure losses, and temperature dependence of specific heats. The result of the validation is that GasTurb 12 is considered a valid tool for design point analysis of two-spool turboshaft systems.

Table 3.2. A sample design point comparison of published example problem results versus results from GasTurb 12 using the same input parameters.

		Example 5.2b		Example 5.3(a&b)		Example 5.3c	
		AS	GT12	AS	GT12	AS	GT12
Temperature (K)	Compressor Inlet	288	288	288	288	288	288
	Compressor Exit	580	579.5	623	621.8	623	621.8
	HPT Inlet	1400	1400	1400	1400	1400	1400
	PT Inlet	--	1164.3	1109	1127.6	1109	1127.6
	Exhaust	751	769.7	815	832.4	823	839.6
	Power (kW)	468.7	476	330	356.2	325.1	347.8
	Thermal Efficiency	0.521	0.474	0.377	0.372	0.368	0.363

AS= Air-Standard Cycle
GS12=GasTurb12

3.3 Hypothetical Off-Design Problem

GasTurb 12 is used to demonstrate its capabilities for a hypothetical off-design problem. Due to a lack of published off-design information, a scenario was devised in order to show how a theoretical gas turbine would behave at off-design conditions. The

example uses the design point established in example 5.3c (as shown in table 3.2) and is operated at a higher ambient temperature. The problem statement is:

> "The gas turbine defined in Example Problem 5.3c has been installed in a desert facility at which the operating temperature is 322 K. Determine the temperature and pressure at each point inside the gas turbine as well as the power output at these off-design conditions. Present the results on component maps which show both the design point and this new off-design point. Furthermore, determine how the gas turbine will operate at part power conditions through an operating line on the same component maps. Finally, provide a plot of thermal efficiency versus shaft power delivered along this operating line."

The results from GasTurb 12 no longer mimic a design point calculation, but rather provide insight into how the gas turbine will operate at 322 K instead of at the design point of 288 K. At this higher inlet temperature, the temperatures and pressures at each point within the gas turbine are higher, and there is less power developed and there is a lower thermal efficiency. This demonstrates typical behavior expected in off-design point operation. The results are shown in table 3.3.

Table 3.3. The results of the hypothetical off-design point example problem alongside the design point.

	Example 5.3c		Off -Design Example	
	Temp (K)	Press (kPa)	Temp (K)	Press (kPa)
Compressor Inlet	288	101.3	322	101.3
Compressor Exit	621.8	1215.9	655.4	1051.8
HPT Inlet	1400	1179.4	1429.2	1019.2
PT Inlet	1127.6	409.8	1158.8	355.9
Exhaust	839.6	102.3	878.1	93.7
Power (kW)		347.8		299.8
Thermal Efficiency		0.363		0.356

Perhaps of greater interest, and certainly a useful tool, are the component maps generated at this off-design point. GasTurb 12 is used to generate maps of the compressor, high pressure turbine, and the power turbine of the two-spool configuration at the off-design design point described in the problem statement. The compressor map is shown in figure 3.2.

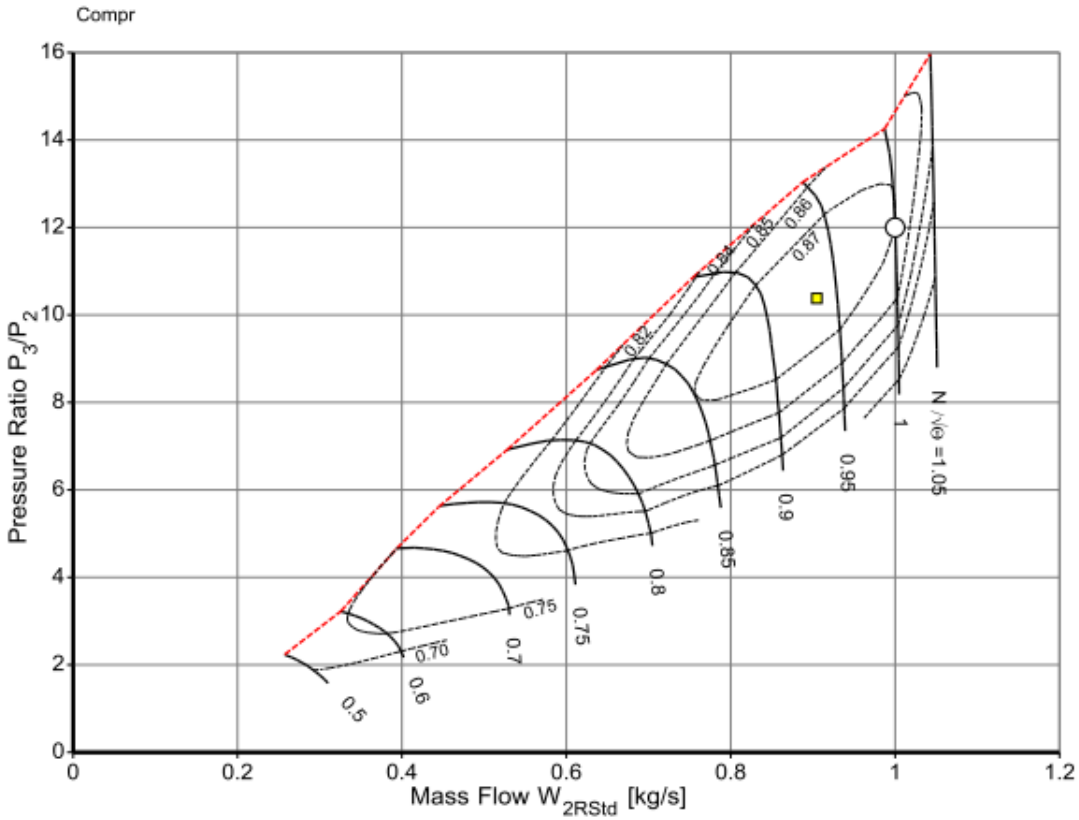

Figure 3.2. The compressor map generated in GasTurb 12. The design point is shown as a circle and the off-design point as a square.

The compressor map gives an idea of how the program controls the turbine. The off-design point does not fall along the same constant corrected speed line as the design point, nor is it nearby, so the compressor does not operate at constant speed. The mass flow rate through the compressor decreases at higher inlet temperatures due to a decrease

in the air density. The compressor has to slow down in order to compensate for the lower mass flow and achieves a lower pressure ratio as a result. The efficiency of the compressor is not greatly affected at this design point.

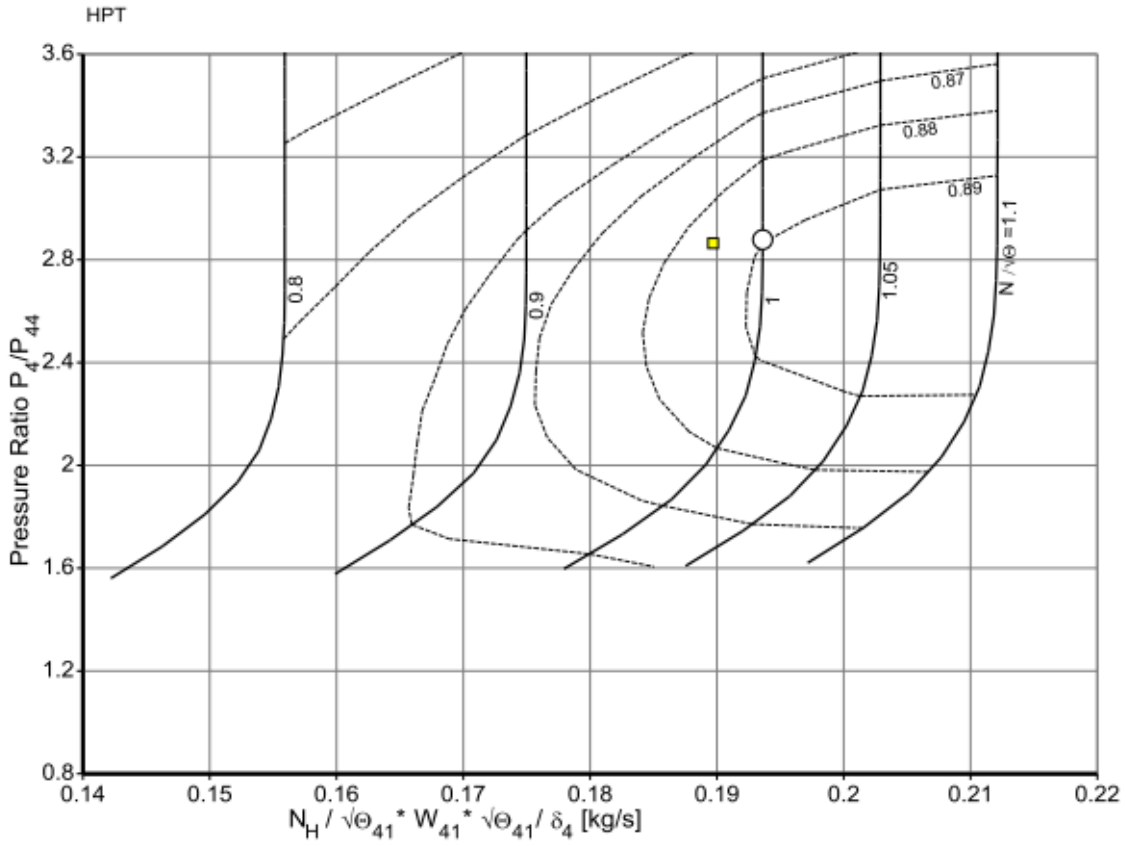

Figure 3.3. The high pressure turbine map generated in GasTurb 12. The design point is shown as a circle and the off-design point as a square. The abscissa quantity is non-dimensional speed times non-dimensional mass flow.

The high pressure turbine map is shown in figure 3.3. The general shape of the turbine map differs from the compressor map, but the observed behavior is approximately the same. As the inlet temperature increases, continuity demands less mass flow also pass through the high pressure turbine. The high pressure turbine is connected to the compressor on a shaft so it rotates at the same speed as the compressor. As the

compressor slows down, so does the high pressure turbine. The result is a point to the left on the turbine map which results in a slightly lower pressure ratio across the high pressure turbine and a slightly lower isentropic efficiency.

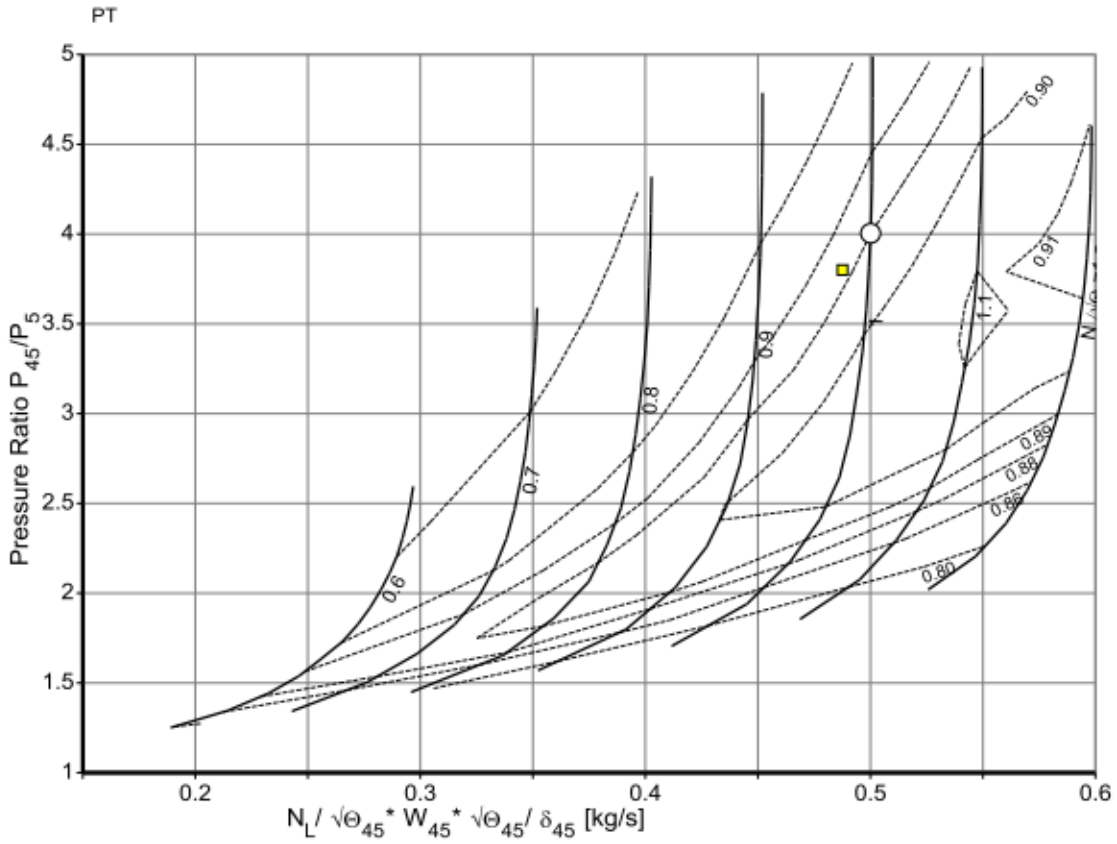

Figure 3.4. The power turbine map generated in GasTurb 12. The design point is shown as a circle and the off-design point as a square. The abscissa quantity is non-dimensional speed times non-dimensional mass flow.

Figure 3.4 shows the power turbine map. It again has a different shape, but the behavior is similar. The power turbine is not connected to the gas generator and is free to rotate at its own speed. GasTurb 12 forces the power turbine to run at a constant 10,000 rpm. This behavior is not readily visible on this turbine map because the off-design point does not lie on the same constant speed line. This is because the constant speed lines

represent non-dimensional speed. As the inlet air temperature increases, non-dimensional speed decreases regardless of the shaft rotation speed. Thus the off-design point falls to the left on the turbine map, off of the constant speed line. The pressure ratio is decreased across the power turbine because the exhaust entering from the high pressure turbine is at a lower pressure than the design point, which can be seen in table 3.3. The exhaust can only expand to ambient conditions across the power turbine so the resulting pressure ratio is decreased at this point.

3.4 Limitations of GasTurb 12

The limitation of using GasTurb 12 for this research is the lack of available modules. The complete program features a diverse toolset, but the free version used here does not. As such, GasTurb 12 can only be used to model two-spool turboshaft systems. Unfortunately, the Arizona State University GTCP85 is a single shaft system which means GasTurb 12 will not be able to accurately model the system. GasTurb 12 can be used to provide a design point comparison, as the design point is independent of geometry, but off-design is greatly influenced by assumed system geometry and GasTurb 12 will not be able to provide reasonable predictions at off-design operating conditions.

4. GTCP85-98D Description

4.1 General Description

The GTCP85-98D in an auxiliary power unit designed for use in aircraft. It is designed to be used as a source of pressurized and heated air, but can also provide shaft power to operate mechanical systems or generate electrical power. The pressurized air is used for jet aircraft starting systems, air conditioning systems, and anti-ice and heating systems. The shaft power output is used to drive generators, pumps, compressors, or other equipment. It can also be used solely as a generator for ground power (Walsh and Fletcher 1998).

The GTCP85-98D features a two-stage centrifugal compressor which achieves a pressure ratio of about 3.25:1. Air exiting the compressor can be bled off into a bleed line to provide pneumatic power, or pass through the combustor and into the single stage turbine. The compressor and turbine are mechanically linked on a single shaft, which also connects an output shaft used to generate shaft power. The output shaft is stepped down through a gear box and the system is controlled to a constant rotational speed of 43,200 rpm (85 Series Auxiliary Power Unit 1969).

4.2 Off-Design Characteristics

The specification curves for the GTCP85-98D provide information regarding the performance of the turbine system for varying inlet temperatures at four levels of shaft

power output. The curves do not provide information for part power operation and do not include any component maps for detailed off-design analysis. Trends are shown in the provided data, but no predictions can be made without additional tools.

It is assumed that because the GTCP85-98D is only rated at maximum power, it is designed to be operated at maximum power while trading bleed air flow rate for shaft power output. This is consistent with the assumptions made in chapter 1 and with the idea that a single spool turboshaft is not optimized to operate at part power conditions.

4.3 Arizona State University GTCP85-98D

Arizona State University has a GTCP85-98D setup in the gas turbine lab at the Tempe campus. The experimental setup is discussed in detail in the following chapter.

5. Arizona State University GTCP85-98D Test Setup

The GTCP85-98D gas turbine located at the Arizona State University Tempe campus has been fitted with an experimental setup by Honeywell. The setup features an array of sensors to measure experimental values throughout the turbine system as it runs and collects data at any point during operation. The test setup is shown in figure 5.1.

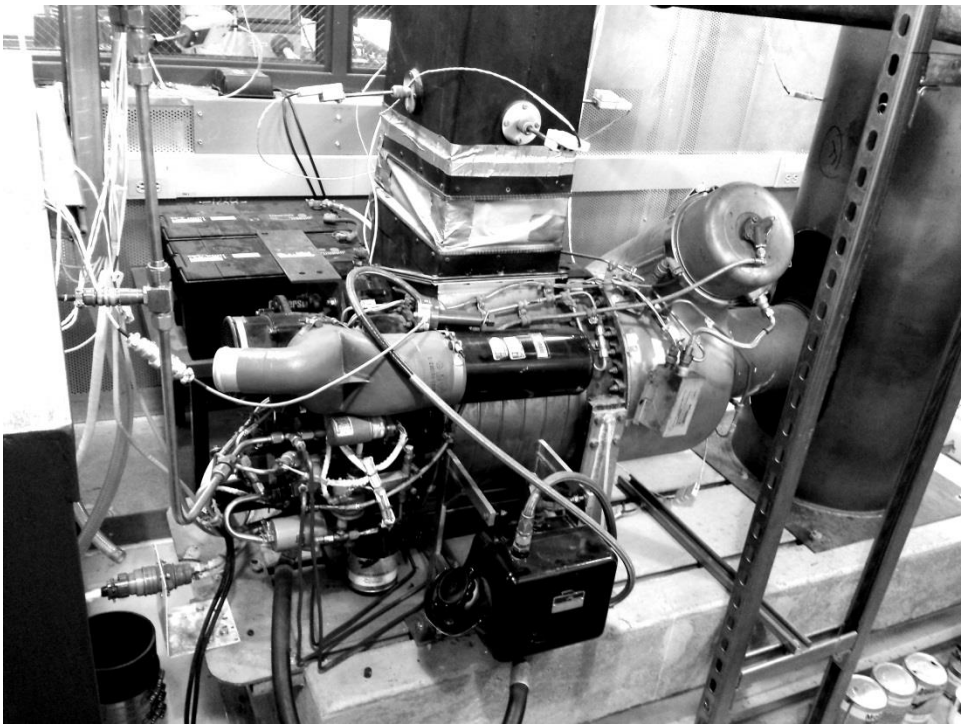

Figure 5.1. The experimental GTCP85-98D test setup at Arizona State University.

5.1 Description of Test Setup

The GTCP85-98D at Arizona State University is located in the engines test lab at the Tempe campus. It resides in an isolated room and is fitted with instrumentation to collect experimental operational data. An inlet stack brings ambient air from outside the

building into the compressor inlet; an exhaust stack carries exhaust from the GTCP85-98D back outside into ambient air; and a series of pipes carries bleed air from the GTCP85-98D through the required instrumentation and then out into the exhaust stack. The rotation speed of the turbine is limited to a constant 43,200 rpm and is stepped down in a gear box so that the output shaft rotates at a constant 6,000 rpm.

An ASME standard long radius, eight inch diameter nozzle is fitted to the inlet duct and is used to measure the volumetric flow rate of air entering the compressor. Another sharp-edged orifice meter is located in the bleed air line and is used to measure the volumetric flow rate of bleed air extracted from the system. Pressure transducers are located at each of the orifices in order to measure the pressure drop across each orifice. A turbine flow meter is used to measure the fuel flow rate.

There are thermocouples located throughout the system to measure temperature at important points throughout the cycle. There is one in the inlet air stream to measure the temperature of inlet air, one at the compressor exit to measure the temperature of air exiting the compressor, one in the bleed line to measure temperature of the bleed air, one in the exhaust stream to measure exhaust gas temperature, and one in the exhaust stack to monitor exhaust stack temperature.

A Froude's dynamometer is fitted to the output shaft and is used to apply a load to the system and to measure shaft power output. It uses a water brake to apply load to the system; the load is increased by increasing the amount of water supplied to the brake. A load cell is fitted to the water brake to measure torque at the output shaft. A tachometer is fitted to the output shaft to measure rotational speed.

The experimental instrumentation is connected to a control panel which feeds data to a data acquisition system. The data acquisition system runs a custom program in Labview and collects and records all the data the instrumentation provides. The Labview program records the values measured by each of the instruments at any given instant as specified by the user. These values are recorded in a spreadsheet which can be exported to Excel as a single document detailing an entire test run. The Labview program records the rotational speed of the shaft, the applied load at the dynamometer, the fuel flow, the ambient pressure, the air inlet pressure drop across the orifice, the compressor discharge pressure, the bleed airline pressure, the bleed air orifice pressure drop, the air inlet temperature, the compressor discharge temperature, the exhaust temperature, the bleed air temperature, and the exhaust stack temperature, all as shown in table 5.1.

Table 5.1. The experimental values recorded at each point by LabView.

Measured Quantity	**Units**
Tachometer	RPM
Dynamometer	ft-lbs
Fuel Flow	lbs/hr
Ambient Pressure	psi
Air Inlet Pressure Drop	psi
Compressor Discharge Pressure	psi
Bleed Air Line Pressure	psi
Bleed Air Orifice Pressure Drop	psi
Air Inlet Temperature	F
Compressor Discharge Temperature	F
Exhaust Temperature	F
Bleed Air Temperature	F
Exhaust Stack Temperature	F

There is additional instrumentation located throughout the system which is used to monitor and to control the system. These instruments are connected to a control panel and monitor the GTCP85-98D as it operates, but do not provide information directly to the data acquisition system. The controlling instrumentation monitors dynamometer water temperature, dynamometer bearing temperature, oil pressure, etc., to ensure nothing goes wrong during a test.

5.2 Test Procedure

The experiment is run for two operating profiles: 1) without bleed air extracted and, 2) with bleed air extracted. The operating profile without bleed air extracted provides shaft power output. The operating profile with bleed air extracted is run with no applied load at the load cell and only provides compressed bleed air. The experimental procedures are detailed in the following sections. The experiment is run first without bleed air and then with bleed air.

5.2.1 Without Bleed Air

1. The GTCP85-98D is started and allowed to fully warm up with no applied load before any data is collected.
2. A data point is recorded with no applied load.

3. The load is increased incrementally and allowed to come to steady state. A data point is collected at each step.
4. The load is increased to the limit of the water brake.

5.2.2 With Bleed Air

1. The water brake is reset to have no applied load.
2. The main bleed air valve is opened. A secondary valve is used to control the bleed air flow rate.
3. Starting with no bleed air flow, the bleed air control valve is opened incrementally to allow an increasing amount of bleed air to be extracted from the system. Data is collected at each increment.
4. The bleed air flow is increased until the exhaust gas temperature reaches 1200 °F.

5.2.3 Notes

It is important to note that the GTCP85-98D is never run at the maximum rated condition in this lab procedure because of two limitations. The first is that the water brake is not capable of providing enough of a load to bring the exhaust gas temperature to the rated value. The second is that the procedure limits the bleed air experiment to an exhaust gas temperature of 1200 °F, not the full rated 1250 °F. None of the datasets examined exceed an exhaust gas temperature of 1160 °F (900 K). The full operating procedure is provided in appendix D.

5.3 Data Collection

At the time of this research, the Arizona State University GTCP85-98D is in a non-operational state. It was intended to run the GTCP85 many times throughout the course of a school year and collect data according to the lab procedure at varying inlet temperatures as the seasons changed. The first attempt at collecting data was unsuccessful because the data acquisition system did not work and no experimental data could be collected. It was then discovered that the water brake could not provide a high load and needed repair.

Fortunately, much of the data collected throughout the years that the GTCP85-98D has been in service at Arizona State University has been saved. The archived data contains datasets collected throughout the seasons and represents a range of inlet temperatures from 70 °F (294 K) to 109 °F (316 K). A total of eight datasets are used in this research.

5.4 Data Comparison

The archived datasets will be used to make a comparison of experimental operation and predicted operation. The bleed data will be used to compare the current operating performance, specifically the off-design performance shown in the experimental data, to the specification curves for the GTCP85-98D. A correlation will be shown from the comparison and the health of the experimental setup will be analyzed.

The no bleed data will be used to compare off-design operating performance with a GasTurb 12 model of the system. A correlation between the off-design performance predictions in GasTurb 12 and the observed performance in the experimental data will be shown. It will be determined if GasTurb 12 can be used to accurately characterize the GTCP85-98D at Arizona State University.

6. Methodology

6.1 Introduction

This research seeks to answer a number of questions as outlined in the introduction (chapter 1). For reference, the research questions are:

1. How well does GasTurb 12 predict off-design point performance of an existing, documented, non-bleed gas turbine?
2. What are the characteristics of a bleed-air APU gas turbine in general, and the GTCP85 specifically, including a cycle model?
3. How does the ASU GTCP85 test data compare with manufacturer's specification values for this engine?
4. Can the current GasTurb 12 software package be used to predict GTCP85 performance to compare with published specification data?
5. How does the ASU GTCP85 test data for no bleed compare with the GasTurb 12 model?
6. What are the next steps to model the GTCP85 with bleed?

In order to best answer the research questions, the research is broken down into three distinct sections. These sections are: an analysis of the LM2500+, an analysis of the published design data for the GTCP85-98D, and an analysis of the experimental data collected from the ASU GTCP85-98D. The analysis and comparison of the LM2500+

data is to establish a correlation between published off-design data and predictions made with GasTurb 12. The analysis of the GTCP85-98D specification data is to evaluate and explain expected off-design behaviors. The analysis of the experimental data collected by the ASU GTCP85 is to establish a correlation between experimental data and an off-design model in GasTurb 12 and evaluate whether or not GasTurb 12 provides a good characterization.

6.2 Analysis of the LM2500+ Data

The data provided in Haglind and Elmegaard (2009) provides all of the necessary input parameters to create a model in GasTurb 12. The basic procedure for the analysis of the LM2500+ data is as follows:

1. Identify standard test measurements for the LM2500+.
2. Use test measurements in the Brayton Cycle Method to determine all input parameters for model in GasTurb 12.
3. Create model in GasTurb 12.
4. Run off-design operating line in GasTurb 12 to form off-design predictions.
5. Record off-design operating parameters in GasTurb12 and compare with the GE data presented in Haglind and Elmegaard (2009).

6.3 Brayton Cycle Method

A Brayton cycle method algorithm is created for the purpose of this research. The purpose of this method is to perform a complex Brayton cycle analysis in order to fill in gaps in experimental data. It is also used to calculate desired cycle outputs, such as generated power, thermal efficiency, and component efficiencies if these values are unknown. The model assumes basic pressure losses, temperature dependence of specific heats, and frictions losses in the components. It uses standard experimental values in order to determine the desired output values. This method is referred to herein at the "Brayton Cycle Method". The algorithm is explained in detail in appendix A.

6.4 Off-Design Point Curves for the GTCP85-98D

The data presented in the GTCP85-98D specification data provides information regarding off-design point performance of the turbine. It does not explicitly state the design point. It is important to first identify the design point and then to identify basic off-design trends and develop a reference plot which will assist someone looking to operate the GTCP85-98D at an off-design point condition. This is accomplished in the following manner:

1. Determine the design point.
    a. Use given values as reference.
    b. Interpolate remaining necessary values.

c. Use Brayton Cycle Method to determine the rest of the design point values.

2. Analyze trends in off-design point data and comment on their behavior. Does this behavior fit expectations? Why or why not?
3. Create an off-design reference curve to show an operator how much bleed air flow he can get for a given shaft power at a given inlet temperature.

6.5 Experimental Data Collected by ASU GTCP85

The data collected by the GTCP85 is analyzed in the following manner.

1. Calculate mass flow rates from pressure drops across orifice plates. The process is described in appendix B.
2. Convert remaining data to SI units.
3. Use the Brayton Cycle Method for every data point.
4. Compare experimental data without bleed air extracted to GasTurb 12 model.
5. Compare experimental data with bleed air extracted to off-design point operating curves.

6.5.1 GasTurb 12 Notes

As previously mentioned, the free version of GasTurb 12 does not contain the necessary modules to model a single spool gas turbine system nor model a bleed air

system. Additionally, the experimental data collected is not collected at the maximum rated EGT condition and cannot be directly compared to the specification data. As such steps 4 and 5 described above are not possible with the current software package. Instead, a commentary is provided to explain observed off-design trends in the experimental data.

7. Results and Discussion

The results of this research are given for each of the three methodologies described in chapter 6. The results begin with the model validation of GasTurb 12 using the LM2500+, continuing to show off-design trends of the GTCP85-98D as predicted by the specification data, and concluding with a discussion of the experimental data collected by the Arizona State University GTCP85-98D.

7.1 Analysis of the LM2500+ Data

The purpose of the analysis of the LM2500+ data presented in Haglind and Elmegaard (2009) is to establish whether or not GasTurb 12 can make accurate off-design point predictions compared to manufacturer off-design data. Haglind and Elmegaard have published a paper which documents the results of a method of off-design prediction and have included data from GE for the LM2500+. The data presented is used to create a model of the LM2500+ in GasTurb 12.

The GasTurb 12 model of the LM2500+ is constructed using a mix of the GE manufacturer's data for the LM2500+ and results of Haglind and Elmegaard's (2009) design point method. They have used a complex cycle analysis in order to determine what turbine inlet temperature, compressor efficiency, and turbine efficiency will result in matching results to the GE data using their analysis method. This design point is shown in table 7.1 under the heading "GE Data & Haglind and Elmegaard". Values in bold are used to create the GasTurb 12 model.

The first step in creating an off-design model with GasTurb 12 is to run a design point with the program. The design point results are shown alongside the results from Haglind and Elmegaard in table 7.1 under the heading "GasTurb 12". The design point results are very similar, except for a slightly increased generator power output. The GasTurb 12 prediction is 3.5% higher. This is attributed to cooling airflows inside the turbine system. In the publication, it is claimed that bleed air is reintroduced into the exhaust flow to cool the turbine blades and the nozzle. This will dilute the exhaust products and result in a lower net power. It is unclear how GasTurb 12 handles bleed air.

Table 7.1 A comparison of the GE Data & Haglind and Elmegaard design point to the GasTurb 12 design point. Values in bold are used to create the GasTurb 12 model.

		GE Data & Haglind and Elmegaard	GasTurb12
K	T_1	**288.15**	288.15
	T_2	768.15	765.37
	T_3	**1523.15**	1523.15
	T_4	-	1127.11
	T_5	806.95	808.5
kPa	P_1	**101.3**	101.3
	P_2	**2360.8**	2361.3
	P_3	-	2290.5
	P_4	-	507.2
	P_5	104.2	104.3
kg/s	$\dot{m}_i$	**88.4**	88.4
	$\dot{m}_f$	1.934	1.963
	$\dot{m}_e$	89.5	89.5
	$\dot{W}_g\ (kW)$	31207	32310.7
	η_{th}	0.377	0.381
	η_c	**0.85**	0.85
	η_t	**0.88**	0.88

An operating line is run using the GasTurb 12 design point model. The operating line describes operating characteristics through a series of power steps, from 10% to

100% power output, using the design point as the reference for the maximum power case. The results are plotted against % load for thermal efficiency, inlet mass flow rate, pressure ratio, and exhaust gas temperature. These plots are then compared to the data presented in Haglind and Elmegaard (2009). Figure 7.1 plots thermal efficiency versus % load.

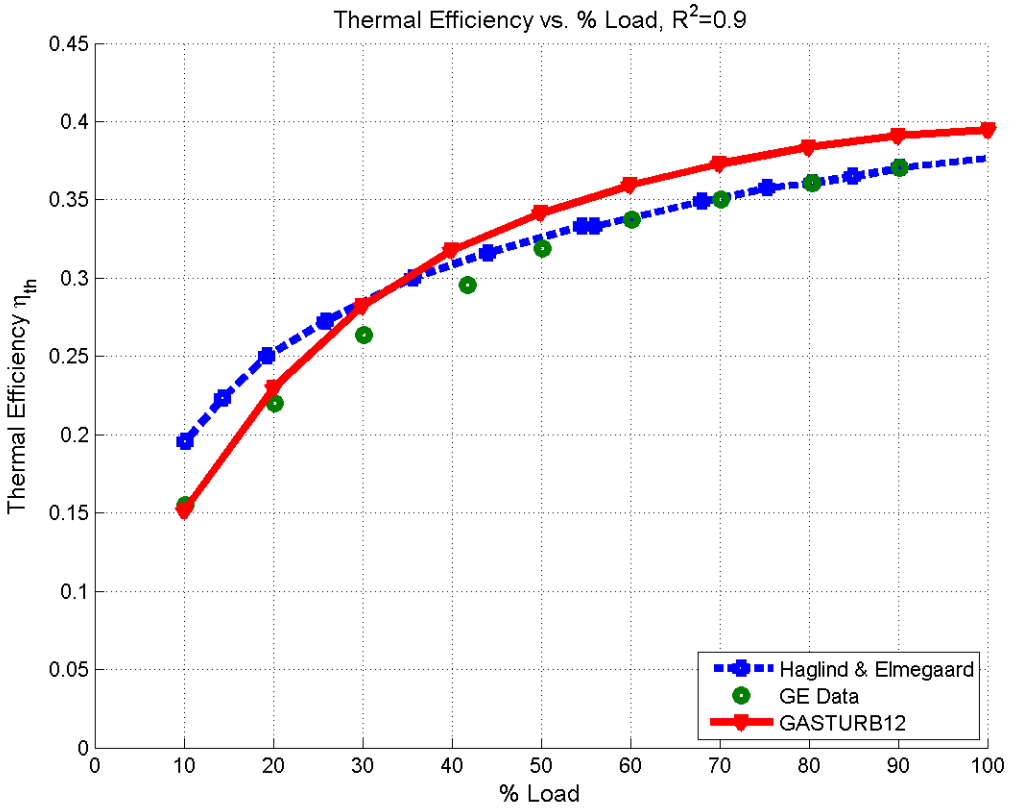

Figure 7.1. Thermal efficiency versus % load for the off-design predictions made by Haglind and Elmegaard, the GE manufacturer's data, and the GasTurb 12 prediction.

The GasTurb 12 predictions fit well with the other data. It is a good fit to the manufacturer's data and there is similar observed behavior in both prediction methods.

The R^2 value represents a goodness of fit of the GasTurb 12 model to the GE Data. It is known as the coefficient of determination and represents how well the model fits the experimental data. The value is calculated using the following formula:

$$R^2 = 1 - \frac{SS_{res}}{SS_{tot}} \tag{7.1}$$

Where:

$$SS_{res} = \sum_i (y_i - f_i)^2 \tag{7.2}$$

$$SS_{tot} = \sum_i (y_i - \bar{y})^2 \tag{7.3}$$

SS_{res} is the regression sum of squares, in which y_i represents a GasTurb 12 value at i and f_i represents a GE Data value at i. SS_{tot} is the total sum of squares in which $\bar{y}$ represents the average of the GasTurb 12 data. The R^2 value is the coefficient of determination. R^2 values range from 0 to 1; an R^2 value of 1 represents a perfect fit. Because the datasets contain a limited number of data points, and the points don't necessarily match the same % load values (or i locations), a fourth-order polynomial is fit to both the GasTurb 12 predictions and the GE Data. This polynomial fit allows for a high resolution calculation of R^2 over the range of 10% to 100% load. This method is used for all R^2 calculations.

The R^2 value of 0.9 in figure 7.1 represents a decent fit to the GE Data. It is not a perfect fit which can be seen in the deviations of the GasTurb 12 prediction from the GE Data, but it is close and maintains shape of the curve. It can be concluded that the fit is sufficient for off-design point predictions as required in this research.

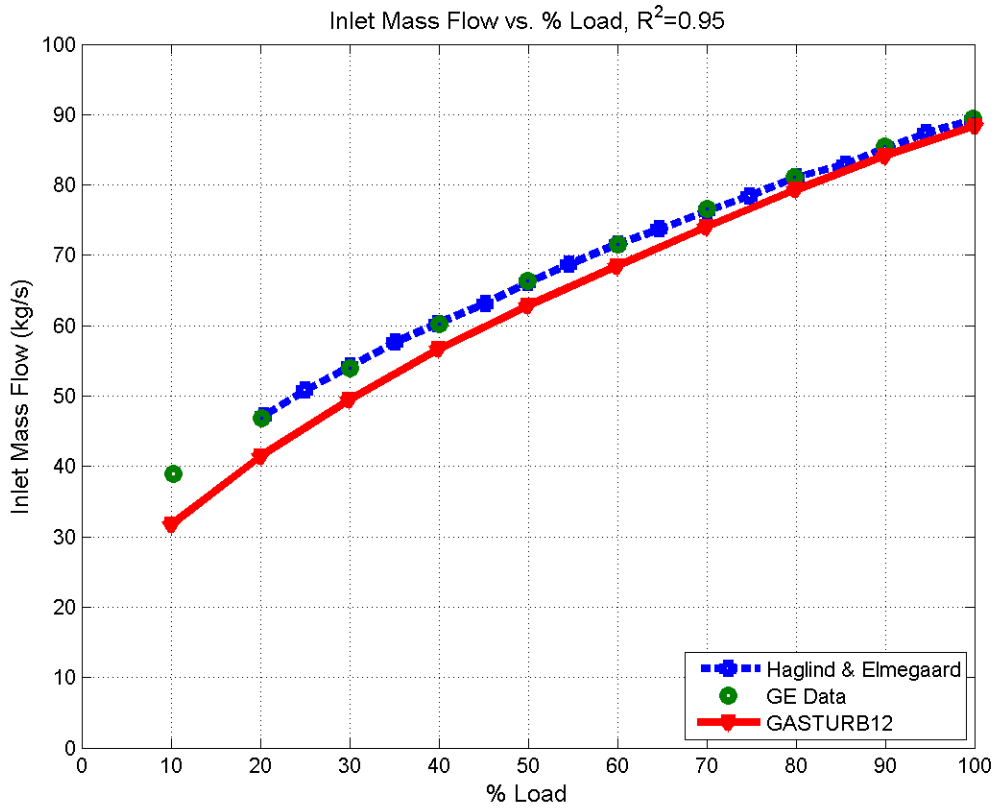

Figure 7.2. Inlet mass flow rate versus % load for the off-design predictions made by Haglind and Elmegaard, the GE manufacturer's data, and the GasTurb 12 prediction.

Figure 7.2 shows inlet mass flow rate plotted versus % load. The R^2 value of 0.95 in figure 7.2 represents a good fit of the GasTurb 12 data to the GE Data. The GasTurb 12 model predicts a low mass flow rate at low % load, but at higher loads, the model is a very good fit to the GE Data. The model provides a good overall fit to the GE data and is sufficient for general off-design point predictions.

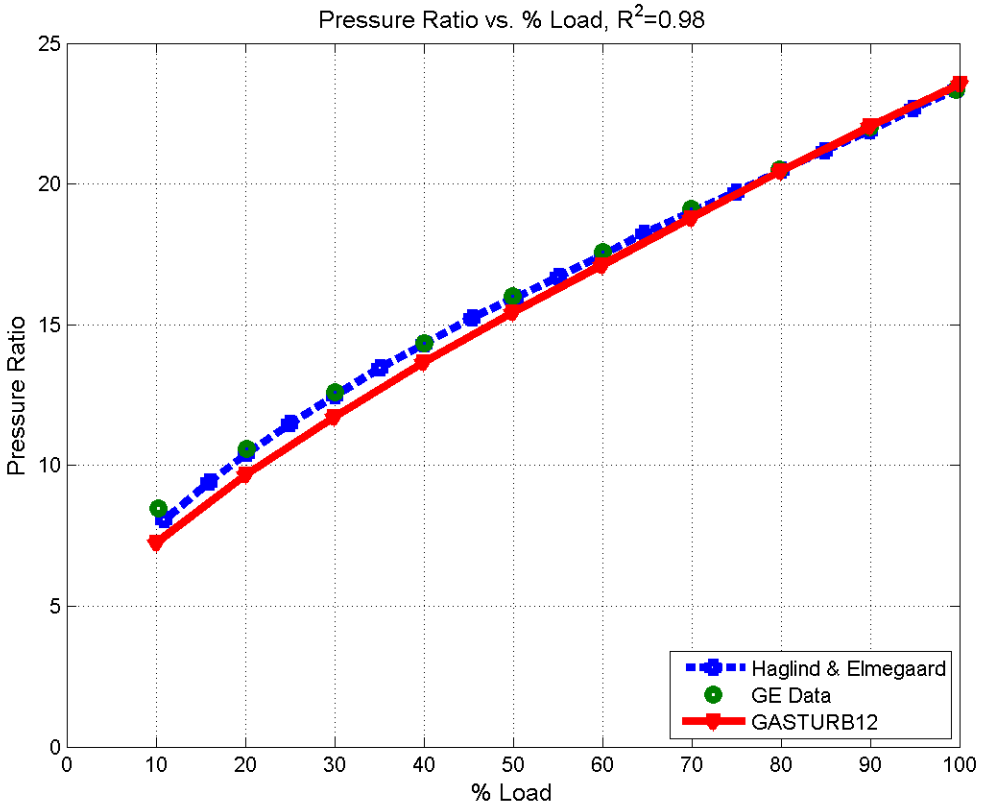

Figure 7.3. Pressure ratio versus % load for the off-design predictions made by Haglind and Elmegaard, the GE manufacturer's data, and the GasTurb 12 prediction.

Figure 7.3 shows a plot of pressure ratio versus % load. The R^2 value of 0.98 in figure 7.3 is a very good fit of the GasTurb 12 prediction to the GE Data. There is very little deviation along the range from 10% load to 100% load and it can be concluded that the GasTurb 12 model very accurately predicts off-design point performance.

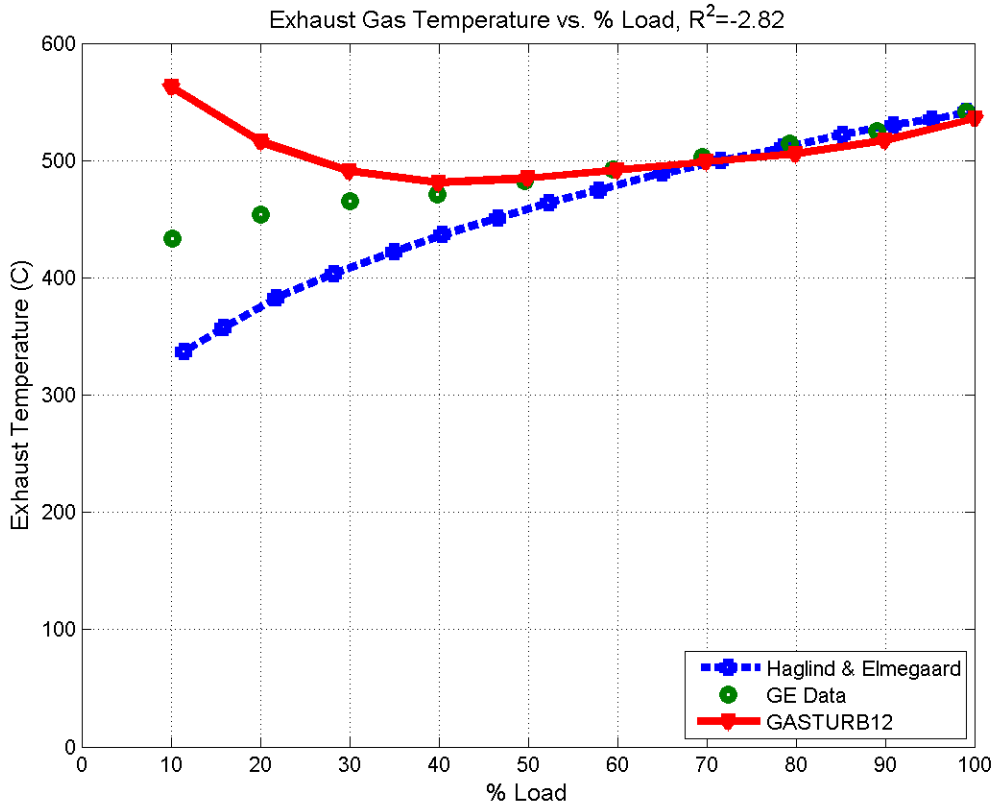

Figure 7.4. Exhaust temperature versus % load for the off-design predictions made by Haglind and Elmegaard, the GE manufacturer's data, and the GasTurb12 prediction.

Figure 7.4 shows exhaust gas temperature plotted versus % load. It shows the only significant deviation from the GE Data to the GasTurb 12 model. At low % load, the GasTurb 12 model predicts high exhaust gas temperatures compared to the GE Data. As % load increases, the prediction becomes much more accurate. This behavior leads to an R^2 value of -2.82. Typically R^2 can only be between 0 and 1, but because this is a non-linear model, R^2 values can become negative. This means the GasTurb 12 prediction is not a good fit to the GE Data for this nonlinear relationship, and this can be confirmed by observing the behavior shown in figure 7.4.

Further observation shows that the fit is improved at higher % load. The polynomial fits are truncated in order remove some of the deviation seen at low % load in an attempt to show a better fit for a higher range of % load. The results are shown in table 7.2.

Table 7.2. R^2 values for different ranges of % load from figure 7.4.

Range (%)	R^2
10-100	-2.82
20-100	-0.63
30-100	0.61
40-100	0.79
50-100	0.75
60-100	0.61
70-100	0.30
80-100	-0.36
90-100	-2.38

Truncating the range shows some effect on improving the fit of the GasTurb 12 prediction to the GE Data. Minor truncations lead to a better fit, but large truncations deviate further from an ideal fit. The best fit is for the range between 40% load and 100% load and is shown in figure 7.5.

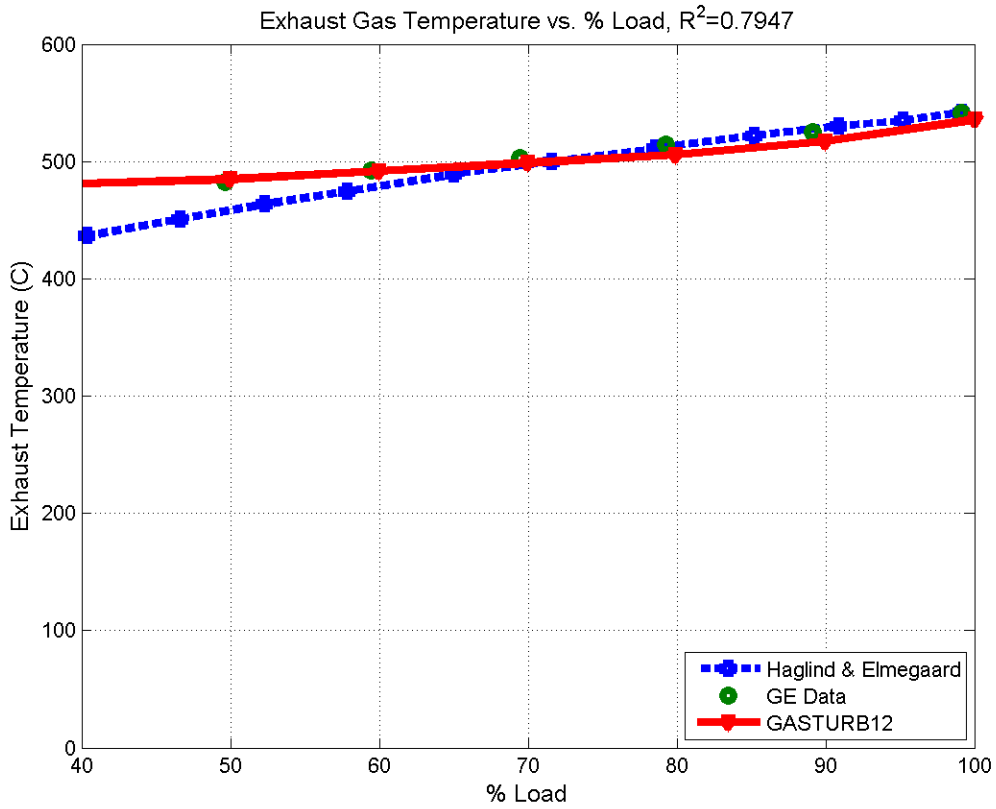

Figure 7.5. Exhaust temperature versus a truncated % load, from 40% to 100% load, for the off-design predictions made by Haglind and Elmegaard, the GE manufacturer's data, and the GasTurb 12 prediction.

The truncated range shows a much better prediction of off-design performance. It is concluded, in general, that GasTurb 12 predicts high exhaust gas temperatures at low % load, but provides good values between 40% and 100% load.

One interesting point to note is that while the GasTurb 12 prediction predicts high exhaust gas temperature, the method described by Haglind and Elmegaard (2009) predicts low exhaust gas temperature. They attribute this behavior to a high prediction of thermal efficiency at part load conditions, which in turn leads to a low exhaust gas temperature. Furthermore, their model includes constant component efficiencies which fail to take into account degradation of component efficiencies at light loads. The

GasTurb 12 model does consider the degradation of component efficiencies at light loads, as shown in figure 7.6.

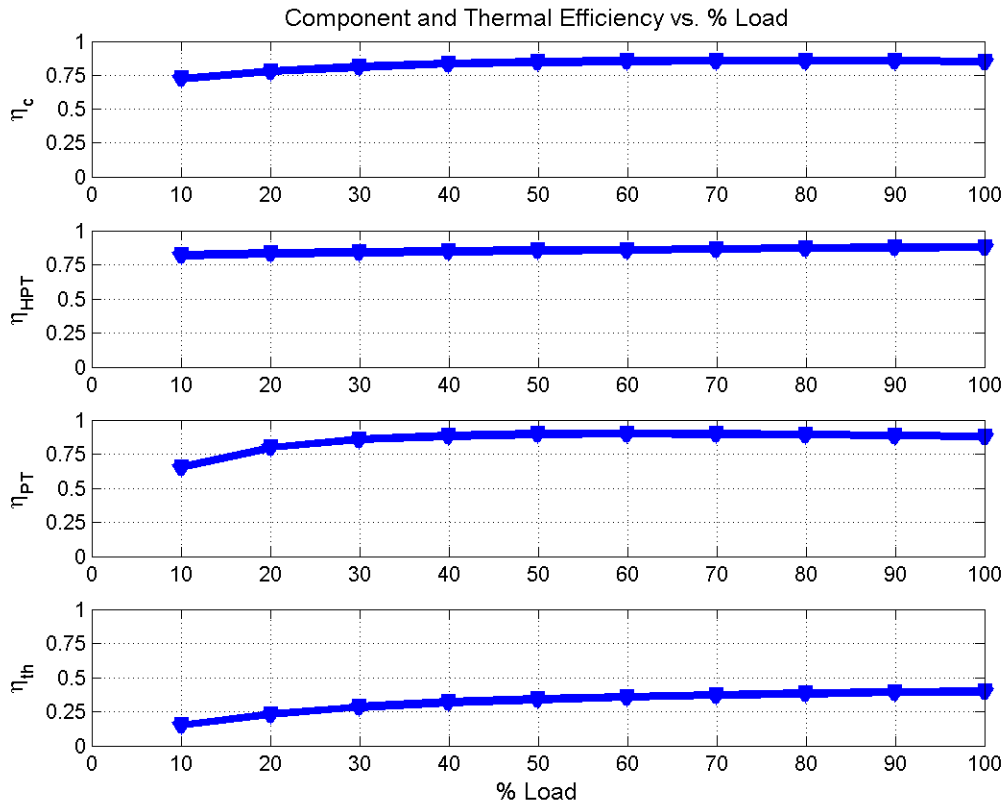

Figure 7.6. Component efficiencies of the LM2500+ from the GasTurb 12 model plotted versus % load. Thermal efficiency is also included for reference.

Figure 7.6 shows nearly steady component efficiency at high loads and clearly shows degradation in component efficiencies at lights loads. The thermal efficiency predicted by GasTurb12 at light loads is shown to be very close to the GE Data in figure 7.1. The deviation in exhaust gas temperature shown in figure 7.3 is not due to deviations in predicted thermal efficiency, but rather the rapid degradation of the power turbine isentropic efficiency at light loads. A low isentropic efficiency will result in a much higher exhaust temperature than a high isentropic efficiency would.

To demonstrate this effect, recall that:

$$\eta_{PT} = \frac{\dot{W}_{PT}}{\dot{W}_{PT,S}} = \frac{\int_{T_5}^{T_4} c_{p,exhaust}\, dT}{\int_{T_{5,S}}^{T_4} c_{p,exhaust}\, dT} \tag{7.4}$$

Using the data from GasTurb 12 at 10% load, $\eta_{PT} = 0.6548$, $T_4 = 929.03\ K$, and $T_5 = 835.64\ K$. From these values, $T_{5,S}$ is determined to be:

$$0.6548 = \frac{\int_{835.64}^{929.03} 0.929+2.46\times10^{-4}T-3.05\times10^{-8}T^2\, dT}{\int_{T_{5,S}}^{929.03} 0.929+2.46\times10^{-4}T-3.05\times10^{-8}T^2\, dT} \rightarrow T_{5,S} = 785.79\ \ K$$

If the η_{PT} didn't experience such a drastic degradation and remained closer to the 30% load value of $\eta_{PT} = 0.8582$, then solving the above equation with these values for T_5 yields:

$$0.8582 = \frac{\int_{T_5}^{929.03} 0.929+2.46\times10^{-4}T-3.05\times10^{-8}T^2\, dT}{\int_{785.79}^{929.03} 0.929+2.46\times10^{-4}T-3.05\times10^{-8}T^2\, dT} \rightarrow T_5 = 806.32\ \ K$$

This shows that by simply avoiding the drastic degradation of the isentropic efficiency of the power turbine results in a $835.64 - 806.32 = 29.32\ K$ lower exhaust temperature. This single calculation isn't enough to explain the much larger deviation, but this effect, combined with similar effects from other component efficiency degradations will lead to a much higher predicted exhaust temperature than the GE Data shows. It is concluded that component efficiency degradation predicted by GasTurb 12 degrade much more quickly at light loads than the well matched components included in the LM2500+.

The results of the GasTurb 12 prediction of the off-design point performance of the LM2500+ show good correlation in general with the GE manufacturer's data presented in Haglind and Elmegaard (2009). Of the four curves presented, three show good correlation between the data, while the fourth shows a deviation that is easily

explained. The GasTurb 12 model provides a good starting point for off-design performance predictions, especially at higher load conditions, and can be considered as a valid tool to perform such an analysis. A more accurate model is needed for more complex predictions and analysis.

7.2 Specification Data for the GTCP85-98D

7.2.1 Design Point

The design point of the GTCP85-98D is undocumented in the specification data. Rather, the specification data documents the performance of the gas turbine for a range of inlet temperatures. These specification curves document off-design performance of the GTCP85-98D, but do not provide an explicit design point of the turbine system. The GasTurb12 model needs a design point in order to create a model for off-design predictions, so it is important to determine this point.

The specification data shows five measured quantities and demonstrates trends in those quantities during off-design operation. The five measured quantities are bleed air mass flow rate, bleed air pressure, bleed air temperature, fuel mass flow rate, and compressor mass flow rate. These five quantities are plotted as a function of inlet temperature for constant values of shaft output power on each plot.

There are two similar data points given along with the specification curves that document the performance of the GTCP85-98D at two given conditions. It is assumed that these conditions represent the design point and although they vary slightly, they are

similar and either can be treated as the design point. The design point of the GTCP85-98D is determined using the conditions given as (2) on the specification curves. The conditions labeled (2) provide the inputs labeled under “Design Point” in table 7.3. The specification curves are provided in appendix C.

The input parameters explicitly given along with the specification curves are incomplete for the GasTurb 12 model, but the rest can be interpolated from the specification curves. Values for the inlet mass flow rate and fuel mass flow rate are interpolated at a shaft output power of 67 Hp, assuming a linear relationship between power outputs. The lower heating value of the fuel is assumed to be 42.798 MJ/kg to remain consistent with the results of the LM2500+ (both use fuels which are approximately equivalent to diesel, or $C_{12}H_{23}$) (Walsh and Fletcher 1998). The ambient pressure is assumed to be a standard value of 101325 kPa. The results of these interpolations and approximations are shown in table 7.3 as “After Interpolation”.

The input parameters interpolated from the specification curves are still incomplete to create a model in GasTurb 12. The remaining parameters are acquired by using the input parameters provided in table 7.3 by using the Brayton Cycle Method. The results are shown in table 7.3 as “After Brayton Cycle Method”.

Table 7.3. The design point input parameters for the GTCP85-98D. Note: the generator efficiency is defined as the shaft power delivered over the net power of the thermodynamic cycle.

Input Parameter	Units	Design Point	After Interpolation	After Brayton Cycle Method
Inlet Mass Flow	lbm/min	-	309.52	309.52
Pressure Ratio	-	3.25	3.25	3.25
Turbine Inlet Temeperature	F	-	-	1717.43
Burner Exit Temperature	F	440	440	440
Lower Heating Value of Fuel	MJ/kg	-	42.798	42.798
Fuel Mass Flow	lbm/hr	-	253.97	253.97
Bleed Mass Flow	lbm/min	91.5	91.5	91.5
Ambient Temperature	F	103	103	103
Ambient Pressure	psi	-	14.7	14.7
Isentropic Compressor Efficiency	-	-	-	0.666
Isentropic Turbine Efficiency	-	-	-	0.884
Generator Efficiency	-	-	-	0.792

The next step is to use the specification data for the GTCP85-98D to create an off-design model in GasTurb 12 and compare it to the specification data. Unfortunately the free version of GasTurb 12 does not have the additional model required for single spool turbine systems and cannot accurately model the GTCP85-98D. In lieu of using GasTurb 12 to model the GTCP85-98D, observations of off-design behavior in the specification data are made to explain off-design behavior of the system.

7.2.1 Mass Flow Rate of Air

The specification data shows that the compressor inlet mass flow rate decreases as inlet temperature increases. This is caused by a change in the air density at varying inlet temperatures. From the ideal gas law, namely:

$$\rho = \frac{P}{RT} \tag{7.5}$$

It is seen that air density is inversely proportional to temperature; that as temperature increases the air density will decrease. The GTCP85-98D operates at a constant speed which means that the volumetric flow rate through the system remains essentially constant. Recall that the relationship between volumetric flow rate and mass flow rate is given by:

$$\dot{m} = \dot{V}\rho \tag{7.6}$$

If the volumetric flow rate remains constant, but the density decreases, the mass flow rate of air passing through must also decrease as temperature increases.

The mass flow rate of bleed air shows the same trend for the same reason. The bleed air removed from the system passes through a fixed geometry orifice. For a constant volumetric flow rate removed from the system, as the air density decreases, the mass flow rate of bleed air removed from the system will also decrease.

As shaft power extracted increases, both the compressor inlet mass flow rate and the bleed air mass flow rate decreases. All of the air which passes through the compressor must have work done on it in order to compress it; regardless of how much bleed air is extracted, the compressor must still compress all of the air passing through. The bleed air extracted is removed after the compressor, does not pass through the combustor, and cannot do work on the turbine. As more bleed air is removed from the system, less air passes through the combustor and turbine, which produces less usable shaft power.

The decrease in mass flow through the compressor as shaft power increases is due to an increase in back pressure. Back pressure is a resistance to fluid flow through the compressor. As shaft power output increases, there is less bleed air being extracted from

the system so more air has to pass through the combustor and turbine. This increased mass flow rate through the combustor and turbine results in an increased resistance to flow through these components. The back pressure prevents additional air from entering the compressor and results in a decrease of mass flow through the compressor at high shaft power output.

7.2.2 Bleed Air Pressure

The pressure in the bleed air line decreases as inlet temperature increases. The increase in inlet temperature leads to a decrease in air density passing through the compressor and results in a lower pressure achieved. This behavior is shown on a compressor map. The GTCP85-98D operates at a constant speed and the behavior of the compressor can be observed along a constant speed operating line. Corrected speed is constant for a given inlet temperature, but varies over the range of inlet temperatures. The design point can be modeled along a single corrected speed line, but deviations from the design point inlet temperature will fall along different corrected speed lines. As inlet temperature increases, corrected speed will decrease. This point will fall to the left on a different constant speed line on the compressor map. This corrected speed line is illustrated by the dashed corrected speed line in figure 7.7.

Recall that corrected flow is defined in equation 1.2. In order to see the effect of temperature remember that non-dimensional flow is proportional to corrected flow. Non-dimensional flow is defined in equation 1.1. As temperature increases, corrected flow will decrease. As corrected flow decreases, the operating point of the compressor will

move to the left along a constant corrected speed. If the constant speed line didn't change with increased inlet temperature, the result would be a higher pressure ratio. However, since the constant speed line will shift to the left as inlet temperature increases, the result is a lower overall pressure ratio. This is illustrated in figure 7.7 along the dashed constant speed line at the point labeled "B". The bleed air is extracted after the compressor, so a lower pressure ratio in the compressor results in a lower pressure in the bleed line.

The pressure of the bleed air increases as shaft power developed increases. There is an increased mass rate of air passing through the compressor and the pressure achieved will be higher. For a constant inlet temperature, corrected flow will decrease as mass flow through the system decreases. As corrected flow decreases, the operating point of the compressor will move to the left along a constant corrected speed line and results in a higher pressure ratio. This point on the compressor map can be visualized by point "C" in figure 7.7. The higher pressure ratio in the compressor will result in a higher pressure measured in the bleed line.

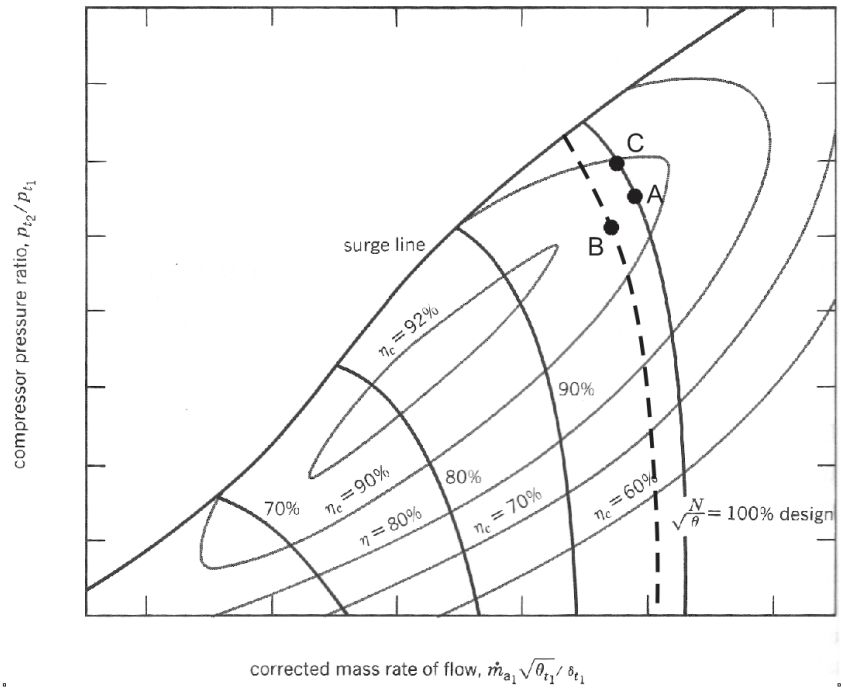

Figure 7.7. A standard compressor map with illustrations. Point "A" represents the design point of the compressor, point "B" represents a point along a lower constant speed line at a lower corrected mass rate of flow, and point "C" represents a point along the constant speed line at a lower corrected mass rate of flow.

7.2.3 Bleed Air Temperature

The bleed air temperature increases as inlet air temperature increases. This is directly related to the increase in inlet air temperature; as warmer air comes in through the inlet it will be warmer when it exits the compressor. Hotter air at the compressor exit will result in hotter air in the bleed line.

The bleed air temperature increases as shaft power delivered increases. Pressure ratio also increases as shaft power delivered increases. A higher pressure ratio will result in a higher temperature at the exit of the compressor, and thus a higher temperature in the bleed line.

7.2.4 Fuel Mass Flow Rate

The fuel mass flow rate decreases as inlet air temperature increases. There is less air mass passing through the combustor which means there is less excess air available to cool temperatures in the combustor. As a result turbine inlet temperature will rise. Turbine inlet temperature is the limiting factor in this gas turbine and has to be controlled. Because temperatures rise with a lower mass rate of air passing through, less fuel must be added in the combustor to achieve the same rated temperature.

The fuel mass flow rate increases as shaft power delivered increases. There is less bleed air extracted from the system as it is exchanged for shaft power and as a result there is more air flowing through the combustor and more fuel must be added to maintain the rated temperature limit.

7.2.5 Operating Curve for the GTCP85-98D

One benefit of understanding off-design performance of the GTCP85-98D is being able to predict how the system will operate at off-design point inlet temperatures. The GTCP85-98D is used as an auxiliary power unit and must provide both electrical power through mechanical shaft output and bleed air pressure. A useful tool to an operator of a GTCP85-98D is a curve which tells the operator how much bleed air flow they may get for a given shaft power output, over a range of inlet temperatures. This curve is not explicitly provided in the specification data so one is made in order to assist an end consumer of the GTCP85-98D. This operating curve is shown in figure 7.8.

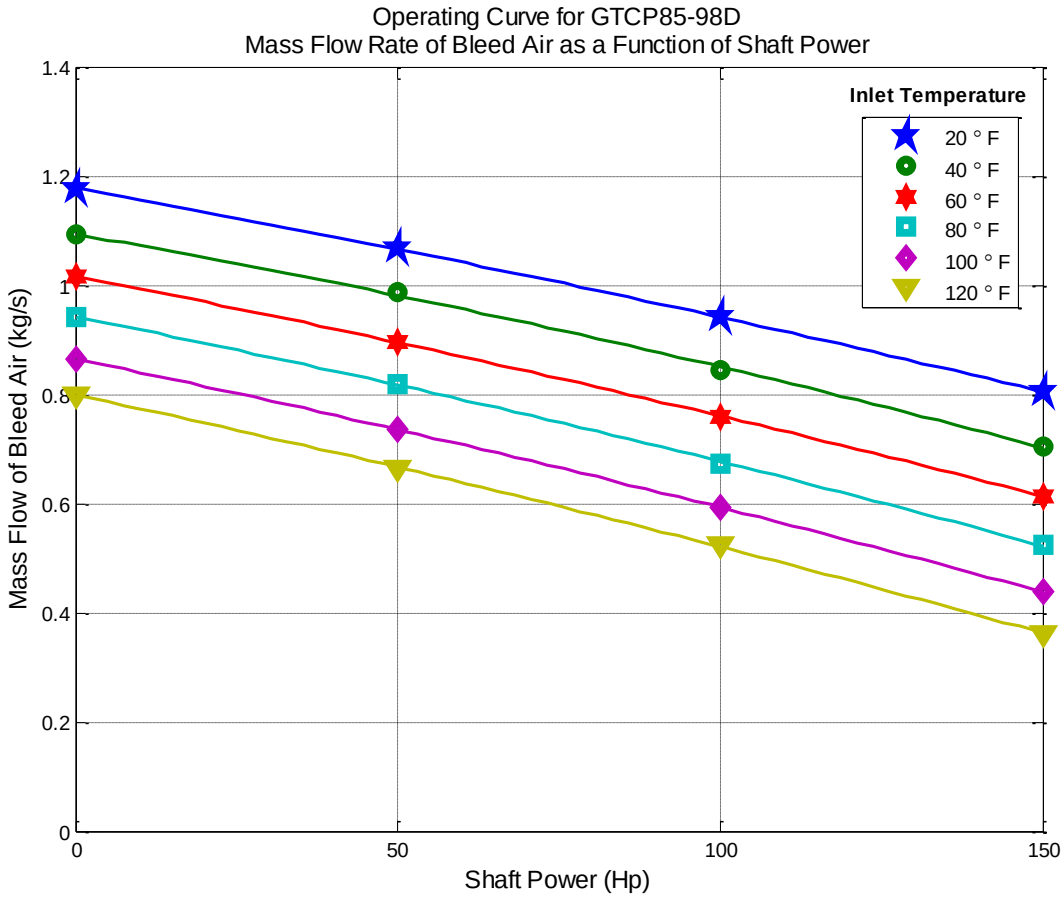

Figure 7.8. The operating curve for the GTCP85-98D. It gives mass flow rate of bleed air as a function of shaft power for a range of inlet temperatures.

7.2.6 GTCP85-98D Off-Design Point Performance Summary

The off-design performance of the GTCP85-98D is result of the many factors at play inside a gas turbine system. The performance shown is expected of the GTCP85-98D single spool gas turbine system at off-design conditions.

7.3 Experimental Off-Design Point Data from the Arizona State University GTCP85-98D

The datasets collected by the Arizona State University GTCP85-98D cannot be directly compared to the specification data because it is collected at part power conditions, whereas it is assumed the specification data is collected at maximum rated power. Instead of a comparison, an evaluation of off-design trends is presented to show behavior of the experimental data and comment on the observed trends.

The data presented is only from the no bleed air part of the experimental procedure. All data collected with bleed air is done with no applied load on the dynamometer and the data is never collected at the maximum rated exhaust gas temperature of 1200 °F. Because there is no shaft powered developed, the data cannot be plotted versus shaft power output similarly to the plots of the LM2500+, nor can it be directly compared to the specification data at 0 shaft horsepower.

7.3.1 Mass Flow Rate of Inlet Air

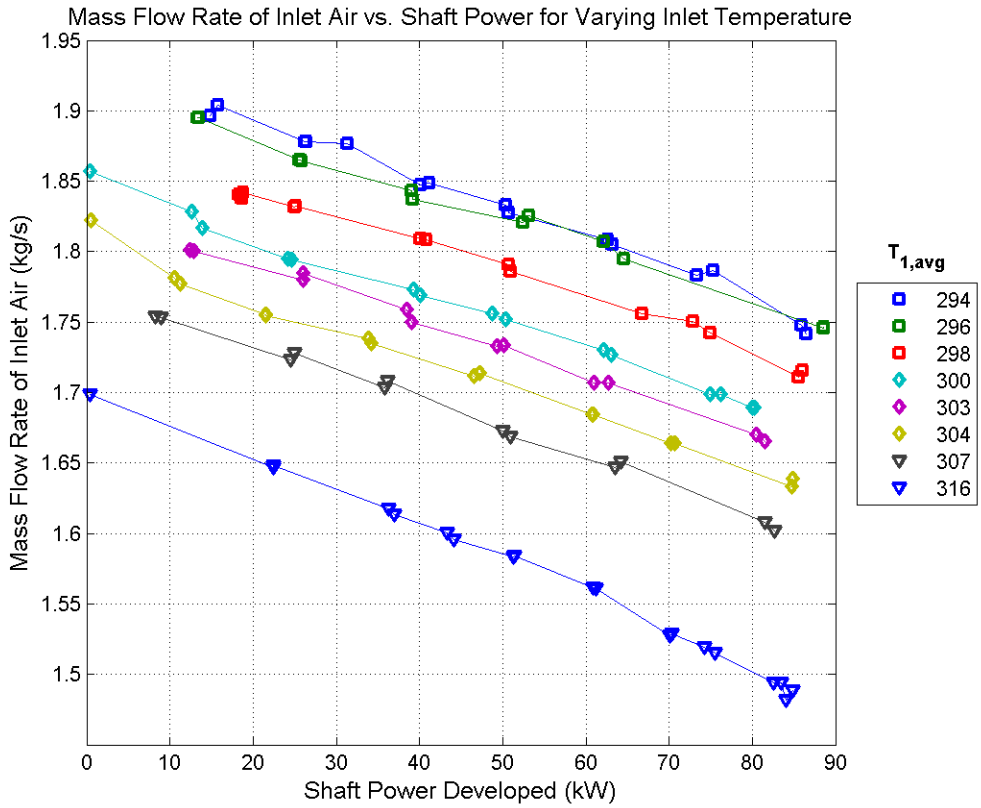

Figure 7.9. Mass flow rate of inlet air through the compressor plotted against shaft power developed for varying inlet temperatures.

The mass flow rate of air through the compressor in the GTCP85-98D is shown in figure 7.9. It shows that as shaft power increases, the mass flow rate of air through the compressor increases. Unlike in the spec data, the increase in shaft power developed is not due to a decrease in bleed air extracted. Rather, an increased load is applied at the dynamometer which results in an increased mass flow rate of fuel into the combustor to compensate. The result is an increased turbine inlet temperature and an increased amount of power extracted through the turbine. The constant geometry of the turbine and the constant spool rate impose a limit so that the exhaust products cannot expand as rapidly

as they would like, and results in a back pressure. The back pressure is an obstruction to air flow through the system and will result in a lower mass flow rate of air through the compressor.

The mass flow rate of air through the compressor decreases as inlet temperature increases. This is due to the decrease in density of the air as inlet temperature increases. The volumetric flow rate of air through the system remains constant so as the density of air decreases, the mass flow rate passing through the system will also decrease.

The mass flow rate of air through the compressor in the GTCP85 shows similar behavior to the spec data. Although the operating conditions are not the same, it is still the same system, mass flow rate of air through the compressor will decrease as shaft power developed increases, and decreases as inlet air temperature increases, even though the operating conditions are different.

7.3.2 Pressure Ratio

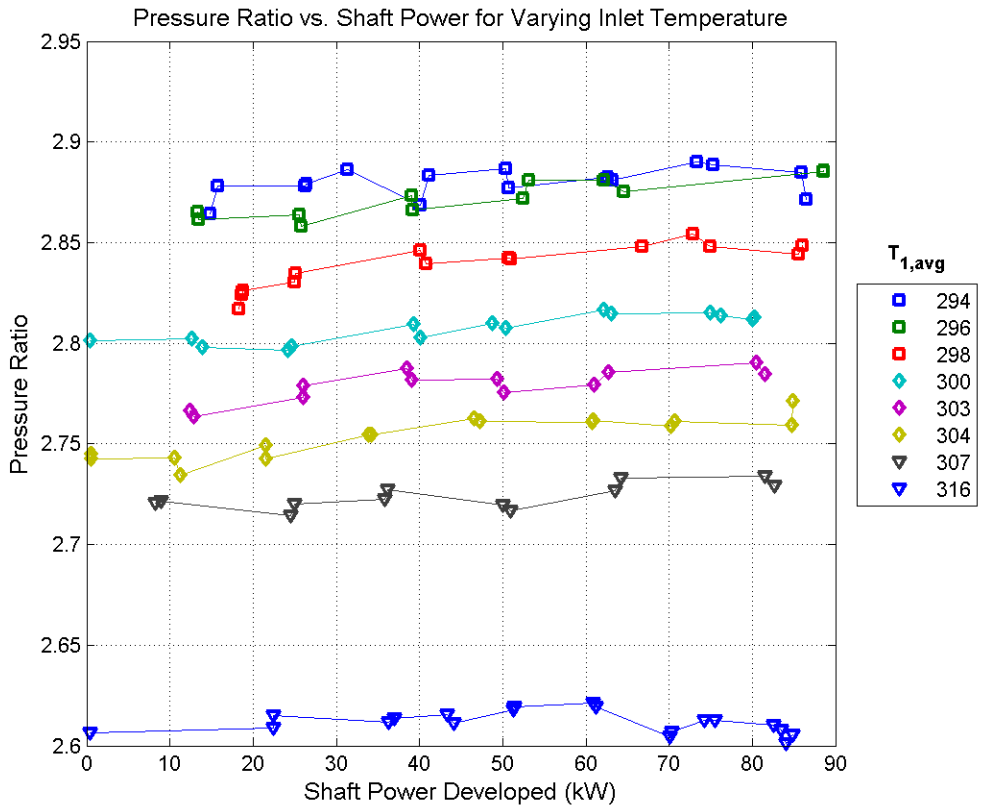

Figure 7.10. Pressure ratio of the compressor plotted versus shaft power developed for varying inlet temperatures.

The pressure ratio of the compressor in the GTCP85-98D is shown in figure 7.10. Pressure ratio increases slightly as shaft power developed increases. Many of the lines appear to be constant, but some of the lines, such as the lines for inlet temperatures of 300 K and 303 K, clearly show a slight increase in pressure ratio as shaft power developed increases. It has already been shown in figure 7.9 that as shaft power developed increases, the mass flow rate of air through the system decreases. The result is an increase in combustion temperature and an increase in back pressure on the system. The back pressure must be overcome and the pressure ratio increases to compensate. As

mass flow rate through the compressor decreases, there is a net decrease in corrected mass flow rate. The increase in pressure ratio for a constant shaft speed is illustrated in figure 7.7 at point “C”.

The pressure ratio of the compressor decreases as the inlet air temperature increases. Air density will decrease and the compressor achieves a lower pressure ratio as a result. The decrease in mass flow through the compressor results in a lower corrected mass flow rate, and it will also fall along a lower constant speed line. This behavior is illustrated in figure 7.11at point “B” and will result in a decrease in the pressure ratio.

The pressure ratio in the compressor of the GTCP85-98D shows similar behavior at part power conditions to the specification data. As shaft power developed increases, the pressure ratio increases; and as inlet air temperature increases, the pressure ratio decreases.

7.3.3 Mass Flow Rate of Fuel

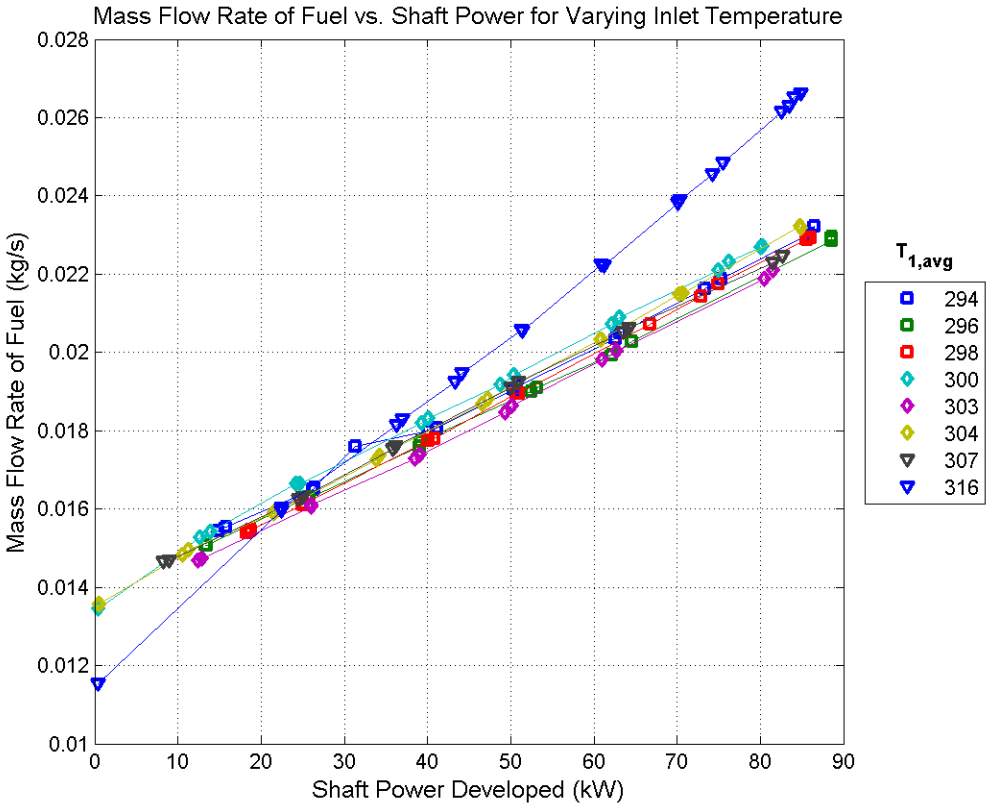

Figure 7.11. Mass flow rate of fuel into the combustor plotted versus shaft power developed for varying inlet temperatures.

Mass flow rate of fuel versus shaft power developed is shown in figure 7.11. The mass flow rate of fuel increases as shaft power developed increases. Power in this experimental procedure is controlled through the fuel flow. As power demands increase, fuel flow must also increase in order to compensate with the increased load.

As inlet air temperature increases the mass flow rate of fuel increases. The density of air passing through the system decreases and inlet air temperature decreases which results in less mass passing through the combustor. More fuel must be burned in the combustor to produce the same amount of work through the turbine.

The trends in the experimental data match the trends in the specification data. The mass flow rate of fuel increases as shaft power developed increases, and increases as inlet air temperature increases.

7.3.4 Exhaust Gas Temperature

While the specification data for the GTCP85-98D is assumed to be collected at the maximum rated exhaust gas temperature, the experimental data collected by the Arizona State University GTCP85-98D is not run at this condition. There is not a constant exhaust temperature so trends in exhaust gas temperature will be analyzed. Exhaust gas temperature as a function of shaft power for varying inlet temperatures is shown in figure 7.12.

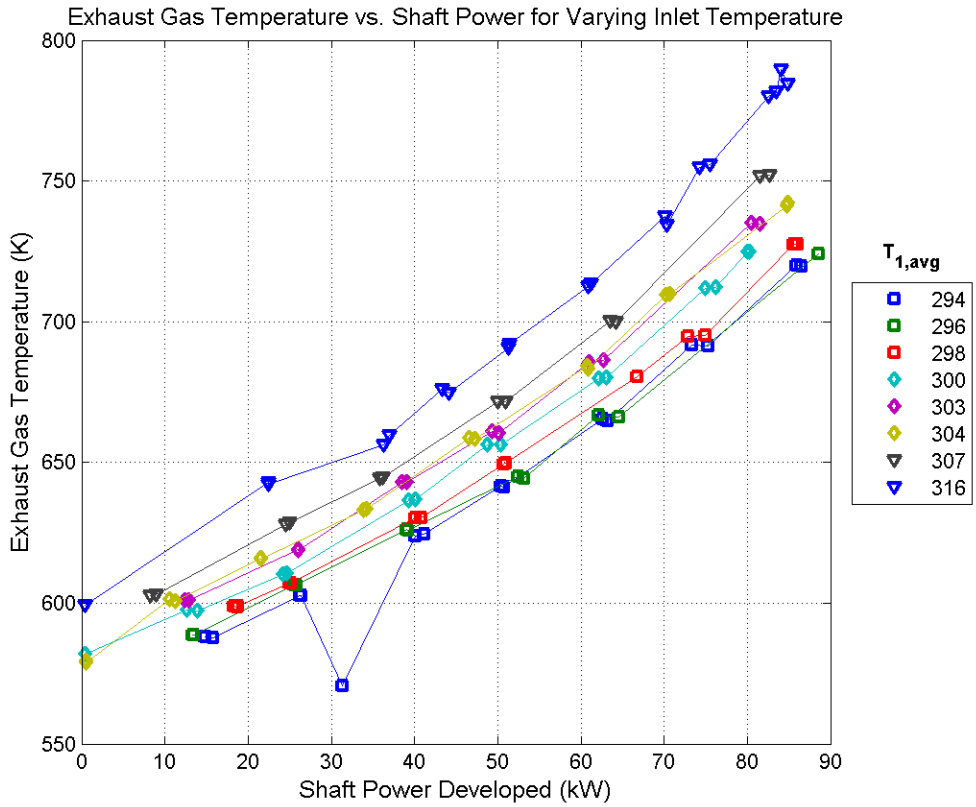

Figure 7.12. Exhaust gas temperature plotted versus shaft power developed for varying inlet temperatures.

The exhaust gas temperature increases as shaft power developed increases because there is increase fuel flow in the combustor. There is more energy released during combustion and the result is a higher turbine inlet temperature. A higher turbine inlet temperature will result in a higher exhaust gas temperature. Exhaust gas temperature is used as a control from this reason. Exhaust gas temperatures are indicative of the turbine inlet temperature and can be easily measured, whereas the turbine inlet temperature is too hot for instrumentation. The GTCP85-98D is limited to an exhaust gas temperature of 950 K (1250 F) in order to keep the turbine inlet temperature in the allowable range.

As inlet temperature increases, there are higher temperatures throughout the gas turbine system. A higher inlet temperature will result in a higher compressor discharge temperature, which will result in a higher turbine inlet temperature, which will finally result in a higher exhaust gas temperature.

7.3.5 Thermal Efficiency

Thermal efficiency in the Arizona State University GTCP85 is calculated as:

$$\eta_{th} = \frac{\dot{W}_{shaft}}{\dot{m}_f LHV} \tag{7.1}$$

This represents the useable shaft power developed by the gas turbine system over the amount of energy added in the fuel. The thermal efficiency of the experimental data is shown in figure 7.13.

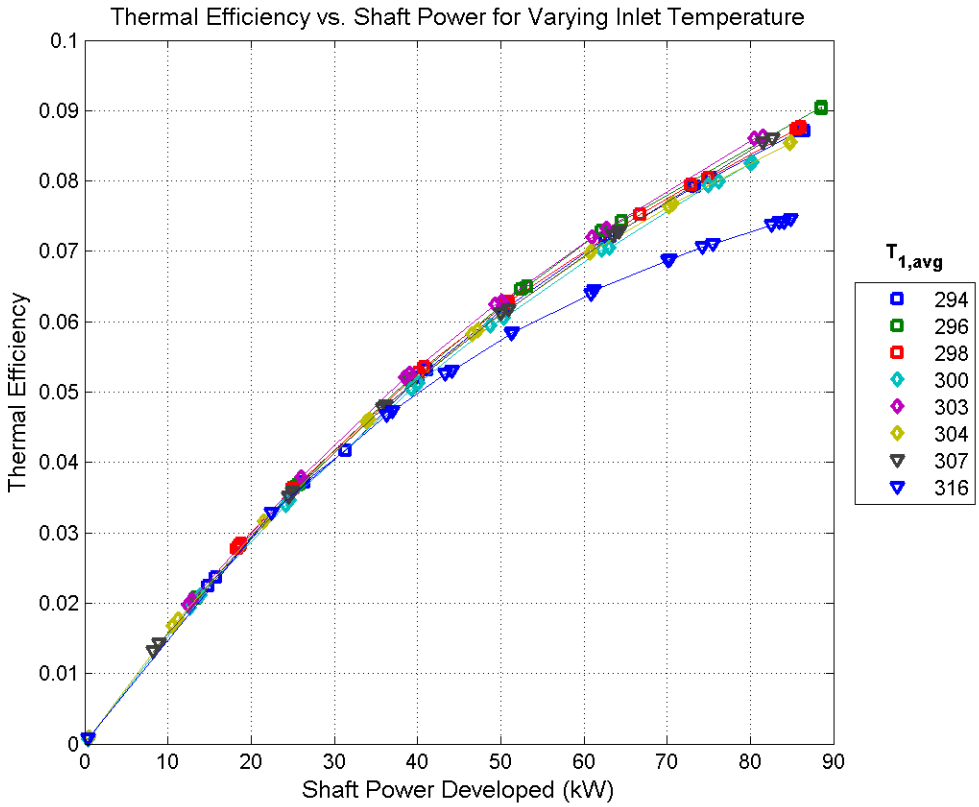

Figure 7.13. Thermal efficiency plotted versus shaft power developed for varying inlet temperature.

The data fits the expected shape of a thermal efficiency curve. As shaft power developed increases, so does the thermal efficiency. The GTCP85 is optimized to run at a maximum rated power and at this point the highest efficiency can be found.

As inlet air temperature increases, thermal efficiency decreases. This is a result of the decreased mass flow going through the combustor and lower component isentropic efficiencies. A lower isentropic efficiency means it takes more power to compress incoming air and less power is extracted from air going through the turbine. Power developed in the turbine is proportional to mass flow through the turbine. The only way to produce the same amount of power at a decreased mass flow rate with lower isentropic

efficiencies is to increase the temperature differential across the turbine by adding more fuel. The result is increased fuel consumption for the same power output, and a decrease in thermal efficiency.

8. Conclusions

Five research questions were stated at the start of this research, and the results and discussions are presented in an attempt to answer these questions. The answers to the research questions are as follows.

8.1 How well does GasTurb 12 predict off-design point performance of an existing, documented, non-bleed gas turbine?

GasTurb 12 is shown to provide good off-design point prediction correlation to manufacturer's off-design data. GasTurb 12 is used to simulate off-design point performance of an LM2500+ and the results have a coefficient of correlation of 0.90 for thermal efficiency versus percent load, 0.95 for inlet mass flow versus percent load, 0.98 for pressure ratio versus percent load, and 0.7947 for a truncated dataset of exhaust temperature versus percent load. It should be noted that the GasTurb 12 prediction provides best results for mid-to-high load ranges and large discrepancies in the coefficient of determination arise from the non-linear behavior of the relationships.

The relevant results and discussion are found in section 7.1.

8.2 What are the characteristics of a bleed-air APU gas turbine in general and the GTCP85 specifically, including a cycle model?

An auxiliary power unit is used in aircraft to assist in main engine starting, supply cooling air, and supply electrical power (Walsh and Fletcher 1998). The GTCP85-98D, in particular, is designed to provide pneumatic power to run jet engine starting systems, air conditioning systems, and anti-ice and heating systems. It also produces mechanical shaft output which can be used to run mechanical systems or generate electricity (85 Series Auxiliary Power Unit 1969).

The GTCP85-98D is a single spool turboshaft system which uses a two-stage centrifugal compressor to compress incoming air, and a single stage turbine to power the compressor and provide shaft power. It can be modeled using a Brayton cycle model, while taking into account pressure losses within the system, accounting for the temperature dependence of specific heats, and considering isentropic efficiency of the components.

The relevant results and discussion are found in chapter 4.

8.3 How does the ASU GTCP85-98D test data compare with manufacturer's specification values for this engine?

The ASU GTCP85-98D test data cannot be directly compared to the manufacturer's specification values. The specification values are generated at a maximum rated condition and the experimental data is not collected at this same

operating condition. The GTCP85-98D is limited by a rated exhaust gas temperature of 950 K (1250 °F) and the specification data is collected at this constant rated exhaust temperature while varying bleed air extraction and inlet air temperature to generate off-design specification curves.

The experimental data collected by the ASU GTCP85-98D is not collected at a maximum rated exhaust gas temperature. Rather, it is collected by varying load applied to the turbine system, and by varying bleed air extracted with no load applied. The result is two dissimilar datasets which cannot be directly compared to provide any good comparison.

The trends in the GTCP85 experimental data are analyzed to show off-design trends and explain their causes. The data shows expected trends as established intuitively from knowledge of the Brayton cycle and analytically, from the specification data. There appears to be no extraordinary behavior in the ASU GTCP85-98D test setup.

The relevant results and discussion are found in chapters 5 and 6 and in sections 7.2 and 7.3.

8.4 Can the current GasTurb 12 software package be used to predict GTCP85-98D performance to compare with published specification data?

The current GasTurb 12 software package cannot be used to predict off-design performance of the GTCP85-98D. The current software package only includes modules available with the free version of the program; the one needed to model the GTCP85 is a single spool turboshaft with variable bleed air extraction and is not included in the free

version of the program. The current software package can be used to model two-spool turboshaft systems, but additional modules will have to be purchased in order to predict off-design performance of the GTCP85-98D.

The relevant results and discussion are found in chapter 3.

8.5 How does the ASU GTCP85-98D test data for no bleed compare with the GasTurb12 model?

The experimental test data cannot be compared to the GasTurb 12 model because there is no module available in the free version of the program to model a single spool turboshaft system. Additional modules will have to be purchased in order to predict off-design performance of the GTCP85 in order to compare a model with the test data.

The relevant results and discussion are found in chapter 3.

8.6 What are the next steps to model the GTCP85-98D with bleed?

The next steps to model the GTCP85-98D with bleed is to acquire additional modules for the GasTurb 12 software package. The free version of the program does not support modeling a single spool turbine with variable bleed air extracted, but there are additional modules available which do. There is ample data available in the specification data and in the experimental data to create a good model and make a detailed comparison between test data and the GasTurb 12 model.

9. Recommendations

It is recommended that additional modules be purchased for GasTurb 12 in order to model a single spool turboshaft system and bleed air systems. This will allow a model to be constructed of the GTCP85-98D in GasTurb 12 and used to predict off-design performance of the turbine. GasTurb 12 has been shown to predict off-design performance with good correlation to experimental data, and it can be further used to model the GTCP85-98D for educational purposes.

It is also recommended that additional data be collected using the Arizona State University GTCP85 in order to better compare the experimental data to the specification values. The current testing procedure does not run at the maximum rated condition and it would be necessary to develop a new procedure in order to collect data at this condition to compare.

REFERENCES

"85 Series Auxiliary Power Unit." Phoenix, Arizona: Honeywell International, Inc., December 1, 1969.

Coefficient of determination. n.d. http://en.wikipedia.org/wiki/Coefficient_of_determination.

Bathie, William W. Fundamentals of gas turbines. New York: John Wiley and Sons, Inc., 1996.

Haglind, F., and B. Elmegaard. "Methodologies for prediction the part-load performance of aero-derivative gas turbine." Energy, 2009: 1484-1492.

Kurzke, Joachim. GasTurb 12: Design and Off-Design Performance of Gas Turbines. Germany, 2012.

Martinjako, Jeremy. Simple Method for Estimating Shaft-Power Gas Turbine Off-Design Point Performance. Tempe: Arizona State University, 2013.

Moran, Michael J., Howard N. Shapiro, Bruce R. Munson, and David P. DeWitt. Introduction to Thermal System Engineering: Thermodynamics, Fluid Mechanics, and Heat Transfer. John Wiley and Sons, Inc., 2003.

Razak, A. M. Y. Industrial gas turbines: Performance and operability. Boca Raton: CRC Press, LLC., 2007.

Walsh, Phillip P., and Paul Fletcher. Gas Turbine Performance. Fairfield: Blackwell Science Ltd, 1998.

APPENDIX A

BRAYTON CYCLE METHOD

Analysis begins with measured data from a gas turbine. The data is representative of a real thermodynamic process with frictional losses. The dataset contains the following measurements:

T_1	Ambient Temperature [K]
T_2	Compressor Exit Temperature [K]
P_1	Ambient Pressure [kPa]
P_2	Compressor Discharge Pressure [kPa]
$\dot{m}_c$	Mass Flow Rate of Air through the Compressor [kg/s]
$\dot{m}_b$	Mass Flow Rate of Bleed Air [kg/s]
$\dot{m}_f$	Mass Flow Rate of Fuel into the Combustor [kg/s]
LHV	The Lower Heating Value of Fuel Burned in the Combustor [kJ/kg]

With the above measured data, a cycle analysis can be performed to determine:

$\dot{W}_{net}$	The Net Work Produced by the Cycle [kW]
η_{th}	Thermal Efficiency of the Cycle
η_c	Isentropic Efficiency of the Compressor
η_t	Isentropic Efficiency of the Turbine

A.1 Cycle Analysis

A gas turbine will have minor pressure losses in the combustor and will have imperfect expansion through the turbine. In order to account for this, it is assumed that:

$$p_3 = 0.97p_2$$

$$p4 = 1.03p_1$$

Which states that there is a three percent pressure loss in the combustor and that air expands through the turbine to three percent higher than the ambient pressure.

In order to determine the net work, the temperature needs to be known at all the state points. Three out of four of these points are known, which leave only T_3 to be determined. A control volume analysis of the combustor shows that air at a mass flow rate of $\dot{m}_2$ at a temperature of T_2 and fuel at a mass flow rate of $\dot{m}_f$ and a lower heating value of LHV enter the combustor. A product of mixed combustor reactants leaves the combustor at a mass flow rate of $\dot{m}_3$ and a temperature of T_3. T_3 can be solved for in the following manner:

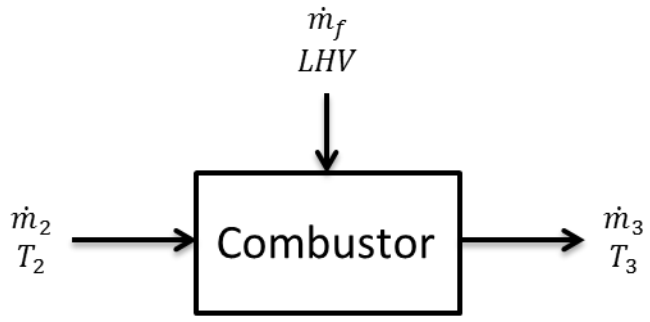

Figure A.1. A control system describing the combustor. Air enters the combustor at a mass flow rate of $\dot{m}_2$ and temperature of T_2. Fuel is added to the combustor at a mass flow rate of $\dot{m}_f$ with a lower heating value of LHV. The exhaust products exit the combustor at a mass flow rate of $\dot{m}_3$ and temperature of T_3.

$$\dot{m}_2 h_2 + \eta_{comb} \dot{m}_f LHV = \dot{m}_3 h_3$$

$$\dot{m}_2 = \dot{m}_c - \dot{m}_b$$

$$\dot{m}_3 = \dot{m}_2 + \dot{m}_f = \dot{m}_c - \dot{m}_b + \dot{m}_f$$

Now since $h = f(t)$, the equation above can be solved for h_3 which will later yield a temperature.

$$h_3 = \frac{(\dot{m}_c - \dot{m}_b) h_2 + \eta_{comb} \dot{m}_f LHV}{\dot{m}_c - \dot{m}_b + \dot{m}_f}$$

Now in order to solve for T_3, recall that:

$$c_p = \frac{\partial h}{\partial T}$$

Thus:

$$h = \int c_p(T) dT$$

In order to evaluate at a given temperature, the integral must be evaluated with respect to a reference value. In this case, the reference value is 0. Thus:

$$h_x = \int_0^{T_x} c_p(T) dT$$

In order to solve for T_3, $c_p = f(T)$ must first be known. A table of values gives relative c_p values as a function of temperature for a variety of different gases. In order to evaluate c_p, the composition of the gases must be known. In this analysis, there are two c_p equations of interest. The first is for dry air, $c_{p,air}$, and the second is for the mixture of combustion products, $c_{p,mix}$. Air is comprised of a mixture of gases, but is primarily composed of N_2 and O_2. A table can be construction showing their relative weights in the mixture that is air, as well as the values from the table. The molar fraction of each gas

will be used to weight its c_p value in order to determine a final equation for $c_{p,air}$. The weighted sum takes the form:

$$c_{p,air} = X_{N_2} c_{p,N_2} + X_{O_2} c_{p,O_2} = 0.79 c_{p,N_2} + 0.21 c_{p,O_2}$$

The result is:

$$c_{p,air}(T) = 0.921 + 2.35 \times 10^{-4} T - 2.80 \times 10^{-8} T^2$$

The combustion product mixture is more complicated because the concentration of each combustion product depends on experimental data and can vary between datasets. First consider the stoichiometric combustion of a hydrocarbon, in this case $H_{12}C_{23}$.

$$C_{12}H_{23} + 17.75(O_2 + 3.76N_2) \rightarrow 12CO_2 + 11.5H_2O + 17.75(3.76N_2)$$

If the combustion is run with excess air:

$$C_{12}H_{23} + 17.75(O_2 + 3.76N_2) + excess\ air \rightarrow 12CO_2 + 11.5H_2O + 17.75(3.76N_2) + excess\ air$$

There will be excess air in the combustion products which will in turn affect the weights of each gas in the c_p. In fact, the exhaust will be made up of mostly excess air. In order to determine how much excess air runs through the system, consider the mass flow rate of air through the compressor and the mass flow rate of fuel. From these, a ratio of molar air to fuel can be determined. In order to do this:

$$\dot{mol}_f = \frac{\dot{m}_f}{MW_f} = \frac{\dot{m}_f}{(12 * 12.011 + 23 * 1.008)} = \frac{\dot{m}_f}{167.32}$$

$$\dot{mol}_2 = \frac{\dot{m}_2}{MW_{air}} = \frac{\dot{m}_2}{28.97}$$

The molar air to fuel ratio is then:

$$AF_{molar} = \frac{\dot{mol}_c}{\dot{mol}_f}$$

This represents the amount of air in moles that pass through the combustor for every mole of fuel burned. From this, the amount of excess air in combustion:

$$excess\ air = AF_{molar} - 17.75$$

So the reaction for the combustor becomes:

$$C_{12}H_{23} + AF_{molar}(O_2 + 3.76N_2) \rightarrow 12CO_2 + 11.5H_2O + 17.75(3.76N_2) + (AF_{molar} - 17.75)(O_2 + 3.76N_2)$$

The mole fraction for each species is then:

$$X_{CO_2} = \frac{12}{12 + 11.5 + 3.76AF_{molar} + (AF_{molar} - 17.75)} = \frac{12}{5.75 + 4.76AF_{molar}}$$

$$X_{H_2O} = \frac{11.5}{5.75 + 4.76AF_{molar}}$$

$$X_{N_2} = \frac{AF_{molar}}{5.75 + 4.76AF_{molar}}$$

$$X_{H_2O} = \frac{AF_{molar} - 17.75}{5.75 + 4.76AF_{molar}}$$

Thus the total $c_{p,mix}$ is a weighted sum:

$$c_{p,mix} = X_{H_2O}c_{p,H_2O} + X_{CO_2}c_{p,CO_2} + X_{N_2}c_{p,N_2} + X_{O_2}c_{p,O_2}$$

Now with $c_{p,air}$ and $c_{p,mix}$ known, T_3 is determined using the following equation and noting that at point 2 there is dry air entering the combustor and at point 3 there is a mixture of combustion products leaving the combustor:

$$h_3 = \int_0^{T_3} c_{p,mix}(T)dT = \frac{(\dot{m}_c - \dot{m}_b)\int_0^{T_2} c_{p,air}(T)dT + \eta_{comb}\dot{m}_f LHV}{\dot{m}_c - \dot{m}_b + \dot{m}_f}$$

This equation is solved numerically to calculate T_3.

Now with the temperature and pressure known at each state point, the net work of the cycle and the thermal efficiency is determined. First the work in both the compressor and turbine is found. The power required to run the compressor is:

$$\dot{W}_c = \dot{m}_c \Delta h_{1-2} = \dot{m}_c \int_{T_1}^{T_2} c_{p,air}(T) dT$$

The work produced in the turbine is:

$$\dot{W}_t = \dot{m}_e \Delta h_{4-3} = \dot{m}_e \int_{T_4}^{T_3} c_{p,mix}(T) dT$$

$$\dot{m}_e = \dot{m}_3$$

And thus the net power produced by the cycle is:

$$\dot{W}_{net} = \dot{W}_t - \dot{W}_c$$

Thermal efficiency is defined as:

$$\eta_{th} = \frac{\dot{W}_{net}}{\dot{Q}_{in}} = \frac{\dot{W}_{net}}{\dot{m}_f LHV}$$

Note that a gas turbine being used for power generation must somehow convert the $\dot{W}_{net}$ of the cycle into usable power. This requires a mechanical setup, with a shaft connecting the power turbine and a generator (or a load cell). There are losses in such a setup which can be accounted for by generator efficiency. This is defined as:

$$\eta_g = \frac{\dot{W}_g}{\dot{W}_{net}} \equiv \frac{\dot{W}_{shaft}}{\dot{W}_{net}}$$

Thermal efficiency must be modified to account for usable power generated, not simply power generated by the cycle. Thus:

$$\eta_{th} = \frac{\dot{W}_g}{\dot{m}_f LHV} = \frac{\eta_g \dot{W}_{net}}{\dot{m}_f LHV}$$

The net power generated by the cycle $\dot{W}_g$ and the thermal efficiency η_{th} are the key results from this analysis. However, the isentropic component effendis can be used to evaluate how isentropic the process is. The isentropic efficiency of a compressor is defined as:

$$\eta_c = \frac{\dot{W}_{c,s}}{\dot{W}_c}$$

Where $\dot{W}_{c,s}$ is the amount of power it would take to compress the air passing through the compressor from P_1 to P_2 if the process occurred isentropically:

$$\dot{W}_{c,s} = \dot{m}_c \int_{T_1}^{T_{2,s}} c_{p,air}(T)dT$$

In order to determine $\dot{W}_{c,s}$, $T_{2,s}$ must first be found. This can be done using the following equation:

$$s_2^\circ = s_1^\circ + \frac{R}{MW_{air}} \ln\left(\frac{P_2}{P_1}\right) = s_1^\circ + \frac{8.314}{28.97} \ln\left(\frac{P_2}{P_1}\right)$$

Where:

$$s_x^\circ = f(T_x)$$

Using tables to determine s_1°, s_2° can be found. $T_{2,s}$ can then be determined by interpolating in the table at s_2°. Thus:

$$\eta_c = \frac{\dot{m}_c \int_{T_1}^{T_{2,s}} c_{p,air}(T)dT}{\dot{m}_c \int_{T_1}^{T_2} c_{p,air}(T)dT} = \frac{\int_{T_1}^{T_{2,s}} c_{p,air}(T)dT}{\int_{T_1}^{T_2} c_{p,air}(T)dT}$$

The isentropic efficiency of the turbine is defined as:

$$\eta_t = \frac{\dot{W}_t}{\dot{W}_{t,s}}$$

Where $\dot{W}_{t,s}$ is the amount of power that would be produced if the gas mixture expanded from P_3 to P_4 isentropically:

$$\dot{W}_{t,s} = \dot{m}_e \int_{T_{4,s}}^{T_3} c_{p,mix}(T)dT$$

In order to determine $\dot{W}_{t,s}$, $T_{4,s}$ must first be found. This can be done using the same method used to find $T_{2,s}$, namely:

$$s_4^\circ = s_3^\circ + \frac{R}{MW_{mix}} \ln\left(\frac{P_3}{P_4}\right) = s_1^\circ + \frac{8.314}{28.97} \ln\left(\frac{P_3}{P_4}\right)$$

Note that the MW_{mix} depends on AF_{molar} and can vary with operating conditions. Thus MW_{mix} can be written as a weighted sum using the same molar fractions used previously:

$$\begin{aligned} MW_{mix} &= X_{H_2O} MW_{H_2O} + X_{CO_2} MW_{CO_2} + X_{N_2} MW_{N_2} + X_{O_2} MW_{O_2} \\ &= X_{H_2O} 44.009 + X_{CO_2} 18.015 + X_{N_2} 28.014 + X_{O_2} 31.998 \end{aligned}$$

Again, $T_{4,s}$ can be found by interpolating in that table at s_4°. Thus:

$$\eta_t = \frac{\dot{m}_e \int_{T_4}^{T_3} c_{p,mix}(T)dT}{\dot{m}_e \int_{T_{4,s}}^{T_3} c_{p,mix}(T)dT} = \frac{\int_{T_4}^{T_3} c_{p,mix}(T)dT}{\int_{T_{4,s}}^{T_3} c_{p,mix}(T)dT}$$

APPENDIX B

GTCP85 EXPERIMENTAL DATA ANALYSIS

Data is collected from the sensors in the GTCP85 experimental setup and yields the quantities displayed in table B.1. These quantities are not all directly usable for analysis and need to be converted into usable quantities. This is done using the following procedure shown in table B.1.

Table B.1 The measured values from the GTCP85 experimental setup.

Measured Quantity	**Units**
Tachometer	RPM
Dynamometer	ft-lbs
Fuel Flow	lbs/hr
Ambient Pressure	psi
Air Inlet Pressure Drop	psi
Compressor Discharge Pressure	psi
Bleed Air Line Pressure	psi
Bleed Air Orifice Pressure Drop	psi
Air Inlet Temperature	F
Compressor Discharge Temperature	F
Exhaust Temperature	F
Bleed Air Temperature	F
Exhaust Stack Temperature	F

B1 Inlet Air Flow Rate

The inlet air flow rate passing through the compressor is calculated using the pressure drop across an orifice located inside of the inlet. The pressure drop is first used to calculate the velocity of the incoming air using:

$$v = \sqrt{\frac{2\Delta P}{\rho}}$$

Where ΔP is pressure drop measured across the orifice and ρ is the density of air. It is important to note that the density of air is a function of inlet temperature and inlet pressure. From the ideal gas equation:

$$\rho = \frac{P}{RT}$$

The velocity is then used to determine the Reynold's Number of the incoming air. This is done using:

$$Re = \frac{\rho v D}{\mu}$$

Where D is the diameter of the orifice and μ is the dynamic viscosity of air. The Reynold's Number is used to determine the discharge coefficient across the orifice using:

$$C_D = 0.19436 + 0.152884\ln(Re) - 0.0097785[\ln(Re)]^2 + 0.00020903[\ln(Re)]^3$$

Finally the mass flow rate of the inlet air can be calculated using:

$$\dot{m}_i = \rho C_D A_o v$$

Where A_o is the area of the inlet orifice.

B.2 Shaft Power

Shaft power is measured as an applied torque to a load cell. The shaft runs at an approximately constant rotation rate, which is also measured. Shaft power can be measured using these two quantities with the relationship:

$$SHP = N\tau$$

Where N is the rotational speed in rad/s and τ is the applied torque in N-m.

B.3 Thermal Efficiency

Thermal efficiency is given as the supplied shaft horsepower divided by the rate of energy added by the fuel source. The relationship is:

$$\eta_{th} = \frac{SHP}{\dot{m}_f LHV}$$

Where $\dot{m}_f$ is the mass flow rate of fuel and LHV is the lower heating value of the fuel.

B.4 All Other Quantities

All other quantities relating to the experimental data are calculated using the Brayton Cycle Method presented in appendix A. For this research, the data containing bleed air has been omitted, so no further analysis is necessary to determine operating parameters with bleed air.

APPENDIX C

GARRETT GTCP85-98D SPECIFICATION DATA AND OPERATING CURVES

GAS TURBINE SPEC DATA

MODEL **GTCP 85-98D**

REVISED ISSUED 12-1-69

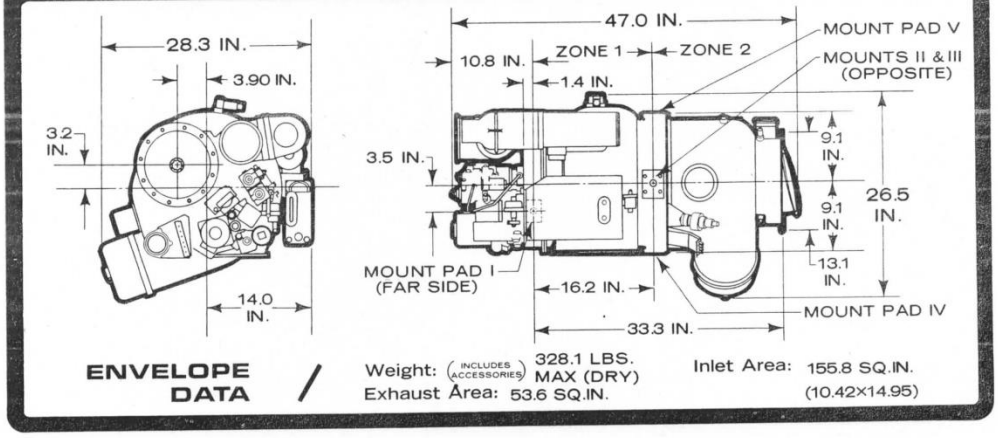

ENVELOPE DATA /

Weight: (INCLUDES ACCESSORIES) 328.1 LBS. MAX (DRY)

Exhaust Area: 53.6 SQ.IN.

Inlet Area: 155.8 SQ.IN. (10.42×14.95)

PERFORMANCE DATA AND LEADING PARTICULARS:

FUELS: MIL-G-5572, MIL-F-5616(JP-1), MIL-T-5624 (JP-4 & JP-5), D1655-63T(JET A, B & A-1)

OILS: MIL-7808D & OTHER AIRESEARCH APPROVED LUBRICANTS

OUTPUT PAD(S): AND 20006, TYPE XII B

DIRECTION OF ROTATION: CW (FACING PAD) 6000 RPM

RATED EGT: 1250°F

ROTOR SPEED: 40,700 RPM

RATING: (FOR INDICATED APPLICATION)

AMBIENT COND.: 103°F SEA LEVEL

BLD. AIR FLOW: (1) 94.0 LB/MIN (2) 91.5 LB/MIN

TEMP: (1) 435±35°F (2) 440±35°F

PRESS.: (1) 47.5 PSIA (2) 47.6 PSIA

PRESS. RATIO: (1) 3.23:1 (2) 3.25:1

SHAFT HP: (1) 60 (2) 67

COMBINATION LOAD: SEE RATING

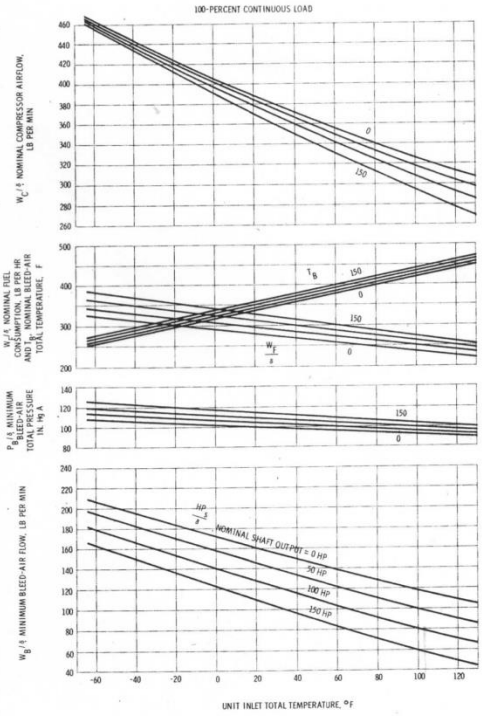

SPECIFICATION DATA:

INSTALLATION DRWG: 380256-1

MODEL SPEC.: SC-5618F

BASIC SPEC: FAA TSO-C77 CAT I CLASS C

APPLICATION: DC9

GARRETT AIRESEARCH MANUFACTURING COMPANY OF ARIZONA, 402 SOUTH 36TH ST., PHOENIX, ARIZONA

MS 1406-37

APPENDIX D

ARIZONA STATE UNIVERSITY GTCP85-98D TEST PROCEDURE

D.1 Gas Turbine Start Up Procedure

1.) Turn on main power to the main control panel (the electrical computer rack).

2.) Turn on computer. Start Labview Program, shortcut on desktop is labeled "Gas Turbine – Instrument Panel".

3.) Check Reset button on wall panel and press if not lit.

4.) Issue ear protectors.

5.) Locate log book

6.) Turn on Maxon Valve located inside 299B. Hold down the orange switch for approximately 15 seconds.

7.) Make sure that the water line's vent valve is closed.

8.) Unplug battery charger and reconnect battery

(Leave battery charger connected to batteries).

9.) Turn on fuel pump. The switch is next to the observation window.

10.) Turn on master switch located on right side of main control panel.

11.) Make sure bleed air valve is closed and system bleed air valve is closed (meter reading 0).

12.) Make sure water to engine is turned off

(Ball valves by window must be closed.)

13.) Start engine. Press the Start switch on main control panel.

14.) Turn on water to water brake bearings. First open the inlet ball valve and then the smaller valve, located by the window.

15.) When the “Ready to Load” (RTL) light, positioned next to the start switch, turns green, the equipment is ready to begin testing.

16.) After start with no load RECORD in log book:

a.) Exhaust gas temperature (EGT).

b.) Oil pressure.

c.) Fuel pressure.

17.) Perform experiment.

18.) At Peak Load for the day RECORD in log book:

a.) Exhaust gas temperature (EGT).

b.) Oil pressure.

c.) Fuel pressure.

D.1.1 Note for Bleed Air Loading Experiment

1.) Bleed air engine valve open.

2.) Adjust system bleed air valve for incremental openings.

3.) Do **NOT** let EGT exceed 1200 ^{o}F.

D.2 Gas Turbine Shut Down Procedure

1.) Close bleed air valves.

2.) Allow engine to cool (EGT ~ 650 ^{o}F).

3.) Master switch off.

4.) Turn off fuel pump.

5.) Turn off water to water brake.

6.) Allow test cell to clear.

7.) Detach battery and plug in battery charger.

8.) Close Labview, shut off computer.

9.) Turn off power to main control panel.

10.) Push cell stop button to close Maxon valve.

11.) Press test cell reset button – leave on.